

Bioencapsulation Innovations

November 2015

CONTENTS

EDITORIAL	1
XXIII Int. Conf. on Bioencapsulation	
IN MEMORY OF	
JEAN-PAUL SIMON	2
2015 PONCELET AWARD	2
FUTURE BRG MEETINGS	5
CALENDAR	12
PUBLICATIONS	15
THESES ABSTRACTS	17
BRG GENERAL ASSEMBLY	30
ARTICLE - PONCELET AWARD	
Microcarriers loaded with bioactive molecules for tissue engineering	3
ARTICLES - BEST CONTRIBUTIONS	
Core-shell hydrogel particles by all-aqueous microfluidics	6
Spherical and elongated micellar carriers as versatile theranostic devices	8
Sonication-assisted layer-by-layer nanoparticles of resveratrol	10
Use of vegetable oils on formulation of efficient bioactive lipid nanocarriers..	13
Production of capsules by coextrusion for colon delivery	18
Fabrication of methacrylate alginate beads for bioencapsulation of cells..	20
Chitosan coating as an opsonization circumvent strategy for plga nanoparticles	22
From co-application to co-formulation of entomopathogenic fungi	24
Spontaneous co-assembly of proteins for encapsulation of a hydrophilic vitamin	26
Control of ultra-high viscosity as a powerful parameter for alginate capsules	28
ASSOCIATION	32

EDITORIAL

XXIII INTERNATIONAL CONFERENCE ON BIOENCAPSULATION Delft, The Netherlands - September 2-4, 2015

The 23th International Conference on Bioencapsulation was organized in Delft in collaboration with Professors-Gabrie Meester and Ruud van Ommen from Technical University of Delft, The Netherlands.



The conference took place in the beautiful site of the TU Delft Science Center. The conference room was just renovated, offering an exceptional setting both for the presentations and coffee breaks.



The attendance counted hundred twenty five researchers coming from twenty seven different countries. Twenty eight industrials and exhibitors attended the conference demonstrating that the conference is more and more attractive, thanks to the high quality of the presented contributions.



Forty oral talks and forty-three posters were presented during the conference. Their associated texts will be soon available on the BRG web site.

The scientific committee selected ten best oral or poster student presentations. Their authors received a diploma and a trophée during the closing ceremony. The abstracts of their contribution are presented in this newsletter issue.



The conference dinner took place at the Lindenhof restaurant and was the opportunity for a lot of informal exchanges.



During the dinner, the 2015 Poncelet award, supported by Procter and Gamble, was attributed to Professor Elena Markvicheva, both for her contribution to microencapsulation and involvement in the BRG network.

The minutes of the General Assembly of the BRG association held during the conference, are included page 30.

Prof. Denis Poncelet
BRG President

TO THE MEMORY OF JEAN-PAUL SIMON

Jean-Paul Simon was one of the co-founders of the BRG who gave an exceptional contribution to the development of our association. He left us on August 4th, 2015. See in tribute of his memory page 2



IN MEMORY OF JEAN-PAUL SIMON

AN EXCEPTIONAL CAREER

Born in 1947 in Leopoldville, Belgian Congo, Jean-Paul Simon moved back to Belgium at the independence of Congo. This beautiful country however marked his whole life.

After a master in chemistry from the Free University of Brussels, with a specialization in biochemistry, he realized a PhD thesis at Ceria Research Institute (Brussels) on Enzyme regulation in *Saccharomyces cerevisiae*. He then joined and realized most of his career at the Meurice Institute (Brussels) where he developed the Biotechnology Unit in 1982. This unit extended

and became the reference in the industrial sector for pilot-scale fermentation, leading to the establishment of the non-profit association Meurice R&D for applied research and support to enterprises. In 2002, Jean-Paul Simon contributed to the creation of IMBP spin-off, specialized in bacterial starters for environmental sector. In 2005 Jean-Paul Simon worked for the creation of the technology incubator Eurobiotec, supported by the Brussels Region. Jean-Paul joined the Eurobiotec team in 2009 until 2012, when he retired but still remained active as consultant (Original Biotechnology Expertize, OBE).



tations at BRG conferences. Co-initiator and co-chair of the COST (European Cooperation in Science and Technology) action 840 then 865, his experience helped to develop the networking inside of the BRG. Largely involved in industrial collaborations, Jean-Paul was one partner of the Bio&Microencapsulation Science and Technology Virtual Institute (European Project Network). In 2013, BRG recognized his exceptional contribution both in BRG activities but also in the microencapsulation field by attributing him the «Life-time achievement Award».



2015 PONCELET AWARD

ONE OF THE BRG LEADERS

In 1990, we was one of the initiator of the Bioencapsulation Research Group and one of his most active members. Organizer for the 1993 International Conference on Bioencapsulation, he was also chairperson and contributor for many BRG events. His group made a large number of oral and poster presen-



BYE JEAN-PAUL

All of his life was devoted to understand how to control bacteria cell metabolism, but he died on August 4, 2015 due to a bacteria over-infection. He was not only a real support for developing the BRG but also one of our best friends.

Prof. Denis Poncelet
BRG President

Supported by Procter and Gamble, the Poncelet Award was created for the 20th BRG anniversary to reward and recognize the contribution of one person to the development of microencapsulation, especially through innovation and support to the Bioencapsulation Research Group.

In 2015, the fifth award was attributed to Professor Elena Markvicheva, from the Polymers for Biology Laboratory of the Shemyakin-Ovchinnikov Institute of Bioorganic Chemistry, Russian Academy of Sciences in Moscow, Russia.

Professor Markvicheva achieved a master degree in Chemistry from Mendeleev University of Moscow. She got her PhD from Shemyakin-Ovchinnikov Institute of Bioorganic Chemistry in 1992 and became full professor in the same institute in 2006.

Professor Elena Markvicheva joined the BRG in 1996. She is a very active

member, promoting actively the association in Russia and more generally in the European east countries.

Professor Markvicheva is Head of Bioencapsulation Group in the Shemyakin-Ovchinnikov Institute of Bioorganic Chemistry, where she run research on microencapsulation applied to biomedical domain. She is the author of more than 300 publications reporting innovative approach of microencapsulation methods, including 7 patents, 8 chapters in books and more than 100 papers.

Professor Markvicheva

developed her career through many national and international collaborations, particularly during stays in Germany, Czechoslovakia, France, Spain, Belgium and Canada .



Dr Johan Smets and Susana Fernandez Pietro (Procter & Gamble), Prof. Elena Markvicheva (Shemyakin-Ovchinnikov Institute), Prof. Ronald J. Neufeld (Queen's University,)

MICROCARRIERS LOADED WITH BIOACTIVE MOLECULES FOR TISSUE ENGINEERING

Markvicheva E¹, Drozdova M¹, Zlobina M¹, Demina T², Akopova T², Grandfils Ch³

INTRODUCTION AND OBJECTIVES

Tissue engineering deals with repair of lost or injured tissues using biomaterials and new cell technologies. Biodegradable polymer scaffolds (films, hydrogels, fibers, microcarriers) are used to support cell growth and proliferation. On the other hand, scaffolds could be also used as growth factor or drug delivery devices to enhance tissue regeneration. Microcarriers (MC) are promising due to their advantages, such as a large specific surface for cell growth and non-invasive injection [Martin et al., 2011]. MC can be designed as multifunctional microbeads, namely they can serve as matrices to support cell attachment and as injectable delivery systems loaded with bioactive peptide to enhance cell growth [Zhu et al., 2008].



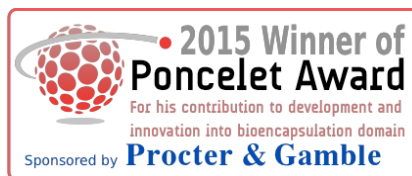
The aim of the study was to develop multifunctional biodegradable polyester-based microcarriers with enhanced surface which are loaded with bioactive peptide to promote cell adhesion, growth and proliferation.

MATERIALS & METHODS

Polyvinyl alcohol (PVA) (Mowiol VP 3-83) was from Hoechst (Germany). Poly(D,L)-lactic acid (PDLLA), Mw 135,000 Da, was synthesized in CEIB, chitosan (Chit), Mw 60,000 Da; DD 90%; Chit-LA and chitosan-gelatin-PLA (Chit-Gel-PLA) copolymers were synthesized by Solid State Reactive Blending technique. Thrombin agonist peptide (TRAP-6, Ser-Phe-Leu-Leu-Arg-Asn, Mw 980) was kindly provided by Dr. Prudchenko (Moscow). All solvents and other chemicals were of analytical grade.

Preparation of microcarriers

MC were prepared by oil-in-water



(O/W) solvent evaporation technique (Privalova et al., 2015). Briefly, an oil phase was obtained by dissolving PDLLA (8%, w/v) in a methylene chloride : acetone (9:1, v/v). The solution was transferred to an aqueous phase containing either PVA (2.5%, w/v) or Chit-LA (2.5%, w/v) and incubated at stirring (500 rpm, 15 C) for 1h. MC modified with Chit-Gel-PLA copolymer were prepared by introducing the copolymer into the oil phase. The MC were settled, washed, and lyophilized. MC fraction of 125– 280 μm was fractionated using metallic sieves and then sterilized by UV irradiation in a laminar flow for 2 h.

TRAP was entrapped into PDLLA microbeads as described earlier (Stashe-

vskaya et al., 2007). MC size distribution was determined using Coulter Counter Multisizer and optical microscopy (Olympus Provis, Japan) combined with an image analysis software (Lucia, Nikon). To modify MC surface by physical adsorption, chitosan was dissolved in sodium acetate buffer (0.3M, pH 4.5), to get 1% (w/v) solution. Then the obtained solution was sterilized (0.2 mm PES filter, Whatman Puradisc, UK), and the aliquots were added to previously sterilized MC (20 mg of MC /200 mL of the polymer solution). After incubation at RT at agitation (200 rpm, 2 h), the MC were washed three times with a steril PBS (pH 7.4) and used for cell cultivation. In case of Chit-LA and Chit-Gel-PLA copolymer added into the oil phase, MC formation and surface modification were carried out at the same time (in one step).

Cell cultivation

Mouse fibroblasts (L929) were culti-

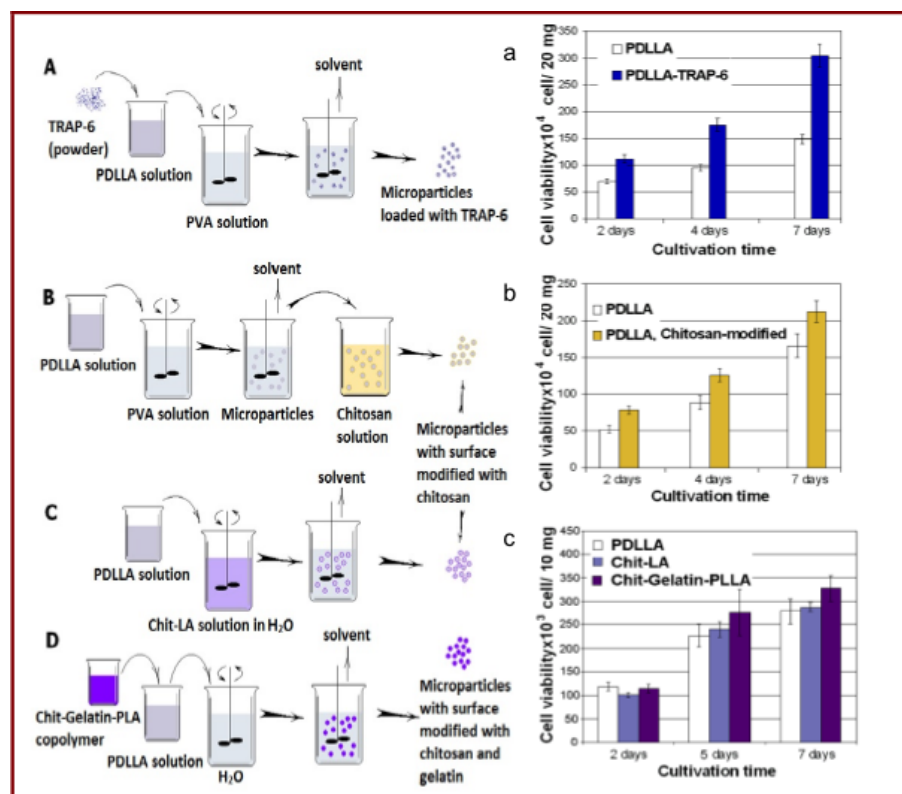


Fig.1. Schemes of microcarrier preparation (A,B,C,D) and cultivation of mouse fibroblasts L929 on PDLLA microcarriers loaded with TRAP-6 (a), or coated either with chitosan (b) or with chitosan-based copolymers (c).

vated in DMEM medium supplemented with 10% FBS in 5% CO₂ humidified atmosphere at 37 °C. The cells were re-seeded into a fresh medium every 2–4 days. Cell culture on MC was performed in 96-well non-adherent cell plates (Sarstedt, Germany) Each well contained 20 mg of MC and 200 mL of DMEM. Initial cell concentration was 5-10 x10⁴ cells/mL of culture medium. Cell viability was calculated by MTT-test.

Characterization of the micro-carriers and cell growth

Scanning electron microscopy (SEM) and confocal laser scanning microscopy (CLSM) were used to characterize MC surface and to control cell attachment and growth on the MC. Freeze-

dried MC were coated with an Au-Pd layer (Sputtering Balzer, SCP-20) and studied using JEOL-840M microscope (A Technics, Tokyo) at a voltage of 19 kV. To study cell growth on the MC, the samples were fixed with 2.5% (w/v) glutaraldehyde solution for 1 h, followed by washing with mQ water and a post-fixation with a 1% (w/v) osmium tetroxide solution for 1 h. Then the samples were sequentially dehydrated in a series of ethanol solutions (30, 50, 75, 95, and 100%) and finally dried by critical point technique.

RESULTS & DISCUSSION

The schemes for preparation of PDL-LA MC are shown in Figure 1 (A, B, C, D). PVA is commonly used as a stabilizer in O/W or O/W/O evaporation

techniques (Fig.1 A). However, as can be seen from Fig. 2, that the cells don't spread well enough at the surface of the MC prepared by this classical technique. Modification of the MC surface with chitosan by its adsorption from the chitosan solution (Fig. 2 B) allows to improve cell adhesion and spreading, and as a result to increase cell proliferation (Fig.1 b). Modification of the MC with chitosan-based copolymers by their addition to water phase (Fig. 1 C) or oil phase (Fig.1 D), respectively, allows to bring chitosan positive charged amino groups to the MC surface. In both cases one can observe better cell spreading (Fig.2), and enhanced proliferation (Fig.1 a and b).

TRAP-6 was earlier shown to promote wound healing in a gastric ulcer rat model (Rusanova et al., 2006). Loading of the MC with TRAP-6 resulted in an increased cell proliferation (Fig. 1 a). On the other hand, surface modification of PDL-LA MC with chitosan also improved cell proliferation (Fig.1 b). However, this first approach when MC surface was coated by polycation sorption from chitosan solution, did not allow us to load TRAP in the microbeads. A low molecular weight peptide was quickly released from the MC (approx. 80% in 2h incubation of the MC in the chitosan solution).

Thus, the second approach can be proposed to get MC with enhanced surface loaded with TRAP-6.

CONCLUSIONS

A novel technique to obtain microcarriers with enhanced surface chemistry has been developed. The modified MC were prepared using 2 approaches, namely 1) coating the MC by chitosan sorption and 2) adding chitosan-based copolymers, in particular Chit-LA or Chit-Gel-PLA, into water or oil phase, respectively, directly at microparticle formation. The second approach allowed to obtain PDL-LA microbeads with enhanced surface chemistry in one step. This simple approach allows to entrap bioactive peptide TRAP-6 in the microcarriers, and therefore, it will be used in the nearest future for that purpose. The modified MC were successfully used to culture mouse fibroblasts L929. Cell behavior (adhesion, spreading, growth and proliferation) on the MC prepared by different techniques was studied by SEM and CLSM. The proposed MC can be promising for tissue engineering.

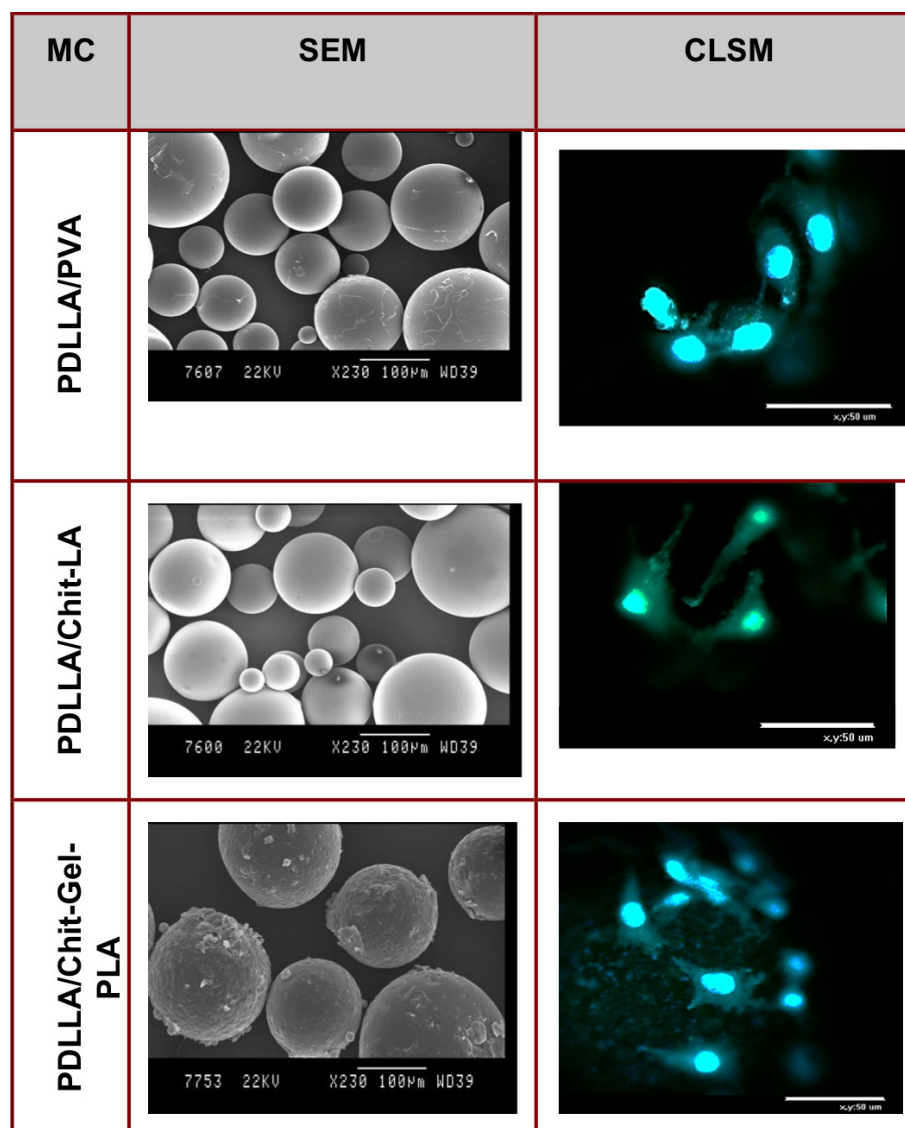


Fig. 2. SEM images of microcarriers and CLSM images of L929 cells growing on them. Cell nuclei are stained with Hoechst (in blue) and cytoplasm of alive cells is stained with Calcein AM dyes (in green).

REFERENCES

- Martin Y. et al. (2011) Microcarriers and Their Potential in Tissue Regeneration. *Tissue Eng Part B*. 17 (1), 71-80.
- Privalova A., Matkviceva E. et al. (2015) Biodegradable polyester-based microcarriers with modified surface tailored for tissue engineering, *J Biomed Mater Res A*, 2015, 103(3), 939-948.
- Rusanova AV et al. (2006) Thrombin receptor agonist Peptide immobilized in microspheres stimulates reparative processes in rats with gastric ulcer, *Bull Exp Biol Med*. 2006, 142(1):35-38.
- Stashevskaya K., Markviceva E. et al. (2007) Thrombin receptor agonist peptide entrapped in poly(D,L) lactide-co-glicolide microparticles: preparation and characterization, *J Microencapsul.*, 24(2):129-142.
- Zhu X. et al. (2008) Delivery of Basic Fibroblast Growth Factor from Gelatin Microsphere Scaffold for the Growth of Human Umbilical Vein Endothelial Cells, *Tissue Eng Part A*, 14 (12), 1939-1947.

Acknowledgement and Full addresses

The study was supported by Russian Foundation for Basic Research (project 14-04-01861).

¹ Shemyakin-Ovchinnikov Inst Bioorg Chem, RAS, Moscow, Russia (le-markv@hotmail.com)

² Enikolopov Institute of Synthetic Polymer Materials,

³ Rus Acad Sci, Moscow, Russia

⁴ Univ Liege, CEIB, Liege, Belgium

**Prof. Elena Markviceva**

Shemyakin-Ovchinnikov Institute of Bioorganic Chemistry
Russian Academy of Sciences
Miklukho-Maklaya 16/10
117997 Moscow - Russia
lemark@mx.ibch.ru ; lemarkv@hotmail.com

19TH MICROENCAPSULATION INDUSTRIAL CONVENTION



Frankfurt, Germany April 4-6, 2016

12 lectures, exhibition

and hundreds of one-to-one meetings

http://bioencapsulation.net/2016_Frankfurt/

8TH TRAINING SCHOOL ON BIOENCAPSULATION



Cork, Ireland - May 30 - June 2, 2016

11 lectures and

3 half days of practical demonstrations

http://bioencapsulation.net/2016_Cork

23TH INTERNATIONAL CONFERENCE ON BIOENCAPSULATION



Lisbon, Portugal - September 21 - 23, 2016

40 oral presentations and
tens of posters

http://bioencapsulation.net/2016_Lisbon/

CORE-SHELL HYDROGEL PARTICLES BY ALL-AQUEOUS MICROFLUIDICS

Mytnyk, S., Totlani, K., Mendes, E., van Steijn, V., Kreutzer, M.T., van Esch, J.H.

INTRODUCTION AND OBJECTIVES

Encapsulation and compartmentalization are crucial to important functions in biological systems and technology, such as controlled release and delivery (Mitragotri, 2012), storage and protection of incompatible components (Nguyen, 2002), and separation. Droplet microfluidics has been shown to be highly efficient method for continuous fabrication of compartmentalized microparticles with unsurpassed control over their structure and contents (Theberge, 2010). Most commonly, they are templated by water-in-oil emulsions, which significantly limits the applicability of this approach for bio- and drugs encapsulation, where presence of organic phases may damage the cargo or increase the toxicity of the formulation. Potential solution to these limitations may be in the use of water-in-water emulsions, formed by so-called aqueous two-phase systems (ATPSs) – immiscible aqueous solutions of two polymers, polymer and a surfactant or polymer and a salt (Hatti-Kaul, 2000). However, due to high viscosities of the polymeric phases and ultra-low interfacial tensions, stable formation of monodisperse droplets generally remains challenging. Typically, additional mechanical actuation (piezo-electric bending, mechanical vibrations etc.) is required to achieve controlled jet break-up, which leads to further complexity of the equipment employed.

Herein, we describe an approach to continuously producing compartmentalized hydrogel microparticles with a liquid core in fully aqueous conditions.

MATERIALS & METHODS

Our method consists of generating a water-in-water double emulsion in a non-planar flow-focusing microfluidic device with a consequent on-chip photo-cross-linking of the shell of the particles (Fig. 1). Previously, we reported the use of a microfluidic device with planar architecture and piezo-electric mechanical actuator to produce monodisperse hydrogel beads

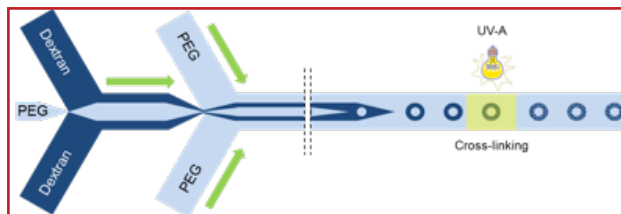


Figure 1. Schematic illustration of the production of core-shell particles..

in fully aqueous system using on-chip polymerization (Ziemecka, 2011).



Aqueous solutions of dextran (MW = 500.000, Alfa Aesar) and poly(ethylene glycol) (PEG, MW = 10.000, Sigma) were used as immiscible phases. Dextrans, constituting the shell, were modified with alkyne and thiol moieties to enable radical cross-linking via thiol-yne photo-“click” (Fig. 2). Alkyne modified dextran (DS = 0.04) was prepared by epoxide opening reaction with glycidyl propargyl ether in basic conditions. Thiol-functional dextran (DS = 0.2) was prepared by carboxymethylation of dextran followed by EDC-NHS coupling to cysteamine. Both polymers were dissolved in 1:1 weight ratio to form dextran phase. All polymeric solutions were filtered using 0.45 μm syringe filters to remove any insoluble impurities and supplied to microfluidic device using syringe pumps (Harvard Apparatus Plus).

For droplet generation, PDMS-based non-planar microfluidic device was employed. It consisted of 2 symmetrically patterned PDMS slabs bonded together after plasma activation. Devices

include two flow focusing junctions, which allowed us to form a jet-in-jet flow. Resulting jet spontaneously broke up into core-shell droplets due to the development of the Rayleigh – Plateau instability and generated droplets were cross-linked by the exposure to UV light (300-400 nm band pass filter) in the presence of radical photoinitiator (Fig. 1). Particles were then collected in a solution of a quenching agent (5% sodium ascorbate) and characterized.

RESULTS & DISCUSSION

Non-planar device architecture was chosen to remove the stabilizing influence of the top and bottom of the channels (partial wetting), which prevented the jet from spontaneous droplet formation previously (Fig. 3). This strategy also minimizes the clogging of the channels, caused by sticking of the particles which were polymerized while in contact with the surface, thus significantly increasing potential operation time of the devices.



We achieved continuous production of core-shell particles: after up to 6 hours of operation, devices did not display any signs of clogging. Core-shell particles of the average diameter of

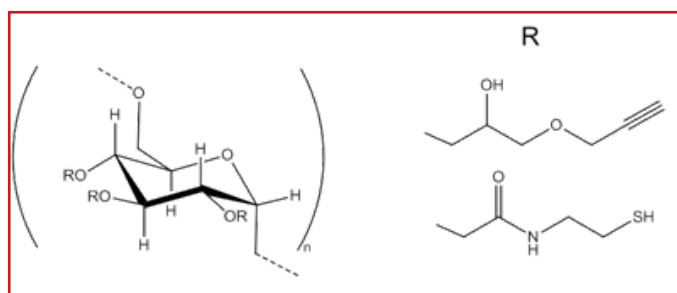


Figure 2. Dextrans for thiol-yne cross-linking.

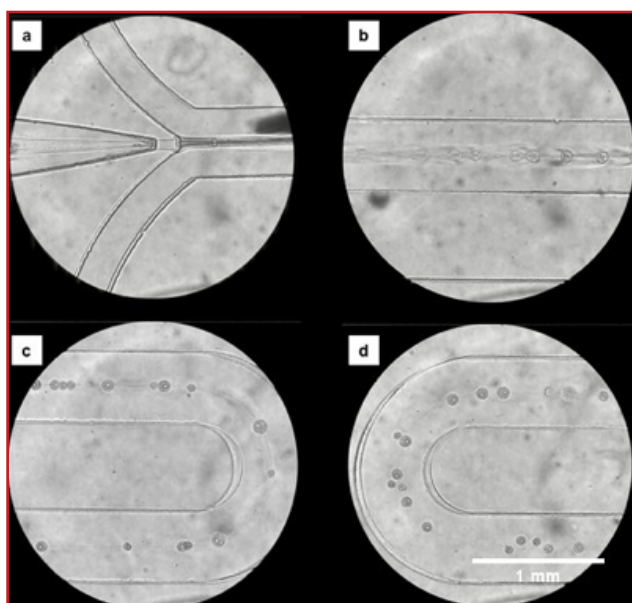


Figure 3. Bright-field microscopy images of the microfluidic device in operation: a) double jet injection into the outer phase, b) break-up of the double jet into core-shell droplets, c, d) fully-formed core-shell droplets.

100 μm were produced. Low interfacial tension of this system allows several different instabilities in the jet to grow simultaneously which leads to higher polydispersity compared to conventional droplet microfluidics.

Due to direct break-up of the double jet into core-shell droplets, instead of a mixed jet, we were able to reduce necessary residence time of the droplets in the device before cross-linking. Such approach also minimizes the possibility of leakage of the contents of the core-phase into the outer PEG flow.

Morphology of the particles was studied using bright-field and fluorescent microscopies (Fig. 4). Particles remained stable in solution for over a month. Drying with consequent rehydration of the particles did not lead to any observable changes. Upon immersion in distilled water particles swelled increasing in size up to 3 times while still retaining their core-shell structure and not displaying any signs of rupturing.

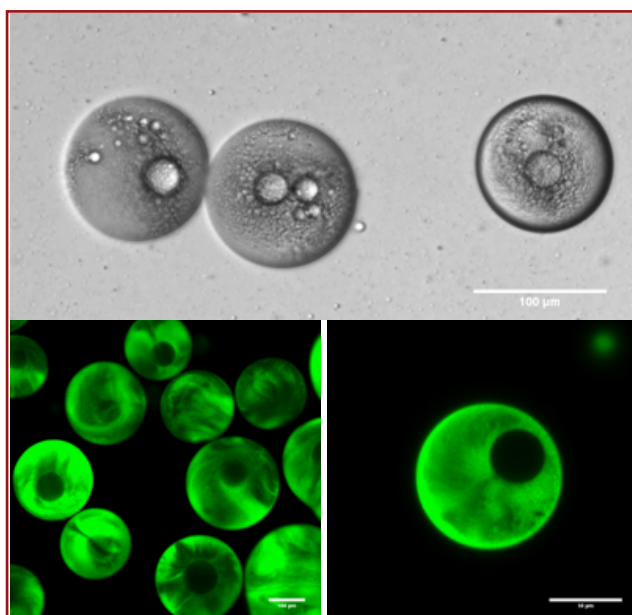


Figure 4. Top – bright-field microscopy image of freshly prepared particles; bottom - CLSM images of core-shell particles; dextran-FITC was added to the dextran shell-phase and is depicted in green. Scalebars: left – 100 μm , right – 50 μm .

Additional tests on the stability of these microhydrogels to harsh external conditions, such as high temperatures, high and low pH and high salinity environments are yet to be performed.

Successful labelling of the separate phases suggests the capability of the method for a controlled encapsulation of the desired cargo in either core or shell. Potentially it should be possible to simultaneously load different objects into the core or the shell of the particles based on their partitioning. Chemical functionality of the dextran hydrogel may also allow covalently binding certain

objects inside the shell thus increasing the selectivity of loading. Additionally, size-dependent release may be possible to achieve by controlling the degree of swelling of these particles, and thus the pore size of the hydrogel network.

CONCLUSIONS & PERSPECTIVES

Here we report an efficient route to continuously producing hydrogel core-shell particles with a liquid core and a permeable shell in fully aqueous environment. This can be potentially used for a controlled encapsulation of biomacromolecules as well as other solutes in mild conditions. We intend to investigate these possibilities in the nearest future.

REFERENCES

- Mitragotri, S. & Lahann J. Materials for drug delivery: innovative solutions to address complex biological hurdles, *Adv. Mater.*, 24, 3717-3723 (2012).
- Nguyen, D. T., Smit, M., Dunn, B. & Zink, J. I. Stabilization of creatine kinase encapsulated in silicate sol-gel materials and unusual temperature effects on its activity, *Chem. Mater.*, 14, 4300-4306 (2002).
- Theberge, A. B., Courtois, F., Schaerli, Y. et al. Microdroplets in microfluidics: an evolving platform for discoveries in chemistry and biology, *Angew. Chem. Int. Ed.*, 49, 5846 – 5868 (2010).
- Hatti-Kaul, R. in *Aqueous two-phase systems: methods and protocols* (ed. Hatti-Kaul, R.), 1-3, (Humana Press, 2000).
- Ziemecka, I., van Steijn, V., Koper, G. J. M. et al. All-aqueous core-shell droplets produced in a microfluidic device, *Soft Matter*, 7, 9878-9880 (2011).

ACKNOWLEDGEMENT

This research was funded by European Commission under Marie Curie ITN SMARTNET (grant 316656).

We would like to acknowledge the contribution of I. Ziemecka, A. Olive and W. van der Meer in the development of this method.



Sehi Mytnyk

Department of Chemical Engineering, Delft University of Technology, Julianalaan 136, 2628 BL, Delft, The Netherlands.

s.mytnyk@tudelft.nl

SPHERICAL AND ELONGATED MICELLAR CARRIERS AS VERSATILE THERANOSTIC DEVICES

Jennings, L.¹, Ivashchenko, O.²⁻³, Laan, A.², Waton, G.¹, van der Have, F.²⁻³, Beekman, F. J.²⁻³, Schosseler, F.¹, Mendes, E.²

INTRODUCTION & OBJECTIVE

The production of nanoparticles is a very active field of research thanks to the plethora of applications for novel nano-sized materials. Full control over the size and morphology of nanoparticles is of fundamental importance for any of their possible applications. In particular, particles which combine a hydrophobic core with a hydrophilic corona are particularly promising for drug delivery applications. Drug molecules, being generally very hydrophobic, can be efficiently encapsulated into the core of these micellar particles. The hydrophilic corona, at the same time, grants water solubility and biocompatibility to the drug-micelle compounds. Moreover, it has been shown that nanoparticles with the right size can passively accumulate within solid tumors thanks to the enhanced permeability and retention effect (EPR) (Fang, 2011). This effect consists in the extravasation of particles that can permeate through the leaky tissue of vascularized tumors.



One of the most promising routes towards simple production of complex nanoparticles is that of polymer self-assembly. By tuning the solvent quality for one of the blocks of a block copolymer, a driving force is generated that pushes the separate unimers to assemble into core-corona supramolecular structures lowering the energy of the system. This is done with small water soluble surfactants which form micelles at equilibrium and also with larger amphiphilic block copolymers. While surfactant micelles are very dynamic systems due to the fast kinetics of these small molecules in water, one can achieve kinetically frozen micellar aggregates using high molecular

weight block copolymers which are not soluble in the destination solvent. The advantage of kinetically frozen micellar aggregates are several: the stability of the structures does not depend on copolymer concentration or, within limits, on temperature. This prevents leakage of entities encapsulated in the core of the micellar nanoparticles. Moreover, due to their out of equilibrium nature, it is possible to obtain very complex morphologies (Zhu, 2008; Cox, 1999)

In this work block copolymers of polystyrene-*b*-poly(ethylene oxide) have been used to prepare micellar carriers of different morphology suitable for radioisotope imaging.

MATERIALS & METHODS

Poly(styrene-*b*-ethylene oxide) block copolymers PS_{9.5k}-PEO_{18k} (Mn/Mw = 1.09) and PS_{9.5k}-PEO_{5k} (Mn/Mw = 1.04) were both purchased from Polymer Source Inc. (Montreal, QC, Canada). The fluorescent dye 1,1'-Diocetyl-3,3,3',3'-tetramethylindocarbocyanine perchlorate (DiI), from Sigma Aldrich.

Micelle formation

The micelles are formed using a co-solvent evaporation method: an emulsion of chloroform-copolymer in water is stirred until the organic solvent evaporates. This causes a copolymer concentration increase in the shrinking emulsion droplets which results in lower surface tensions between the solvents and finally in a critical formation of nanocarriers as a way to change the surface to volume ratio. Fluorescently labelled nanocarriers were prepared by dissolving the dye DiI in the chloroform-copolymer stock solution.

Spherical micelle characterization

The intensity weighted particle size distribution and average hydrodynamic radius of the spherical micelles were obtained by Dynamic Light Scattering (DLS). Each micelle sample was diluted to a concentration of 0.1 mg/mL and measured using an ALV/DLS/SLS-

5020F experimental setup (ALV Laser Vertriebgesellschaft mbH, Langen, Germany) with a He-Ne laser (22 mW, $\lambda_0=632.8$ nm), a compact ALV/CGS-8 Goniometer system, and an ALV-7002 autocorrelator.

Elongated micelle characterization

The diameter and length of the elongated micelles was determined by scanning electron microscopy. Droplets of 10 μ L of micelle solution were diluted to 0.1 mg/mL and spincoated onto 5x5 mm silicon substrates. These were imaged using a SU8000 Ultra High Resolution Cold-Emission FE-SEM Scanning Electron Microscope (Hitachi). The samples were imaged at 1kV acceleration voltage and without applying any conductive coating to the sample.

The length distribution of the elongated micelles was reduced using a homogenizer (Ultra Turrax IKA basic T10). Each sample of 2.3 mL was homogenized at 30k RPM for 30 seconds in total.



Radiolabelling

A solution of 2.3 mL PBS (pH 7.4) and 1 mM tropolone is prepared. The required amount of ¹¹¹In is added to this aqueous solution and the solution is stirred using a glass coated magnetic stirring bar for 5 minutes to allow the formation of tropolone ¹¹¹In complexes. A 100 μ L aliquot of polymer stock solution is added and an emulsion with water is formed by stirring the two immiscible solvents with a glass magnetic stirring bar. The emulsion is kept mixing until all the chloroform has evaporated.

Purification of the micelles from unencapsulated and uncomplexed tropolone and ¹¹¹In was done by size exclusion chromatography using Sephadex® G-25 gel. Elution fractions

ARTICLE

are collected and the activity of each one is counted in a 2480 Wizard2 Automatic Gamma Counter (Perkin Elmer).

Animal handling

Animal experiments were performed with C57Bl/6 mice according to protocols approved by the Animal Ethical Committee of the UMC Utrecht and in accordance with Dutch Law on Animal experimentation. SPECT/CT imaging was used as a noninvasive method to access circulation dynamics and tissue deposition of ^{111}In -labelled micelles.

Six mice were divided into three study groups of two animals and assigned for imaging with sPSL, sPSS or ePSS ^{111}In -labelled micelles respectively. All animals were anesthetized with isoflurane and injected with activity via a tail vein. Average injected activities per study group were 1.45 MBq (1.5 mg) ^{111}In -sPSL, 0.26 MBq (1.8 mg) ^{111}In -sPSS and 0.42 MBq (1.5 mg) ^{111}In -ePSS respectively. After this, total body SPECT/CT scans of 30 minutes were acquired at just after the injection, 24 and 48 hours post-injection (p.i.).

RESULTS & DISCUSSION

The micelles were loaded with a fluorescent probe in order to follow their internalization in HeLa cells. The internalization of the micelles within the cells was evaluated from confocal microscopy images. It was found that the elongated micelles, although through a slower uptake path, are able to deliver more dye to the cells within 24 hours of incubation.

In order to evaluate the biodistribution of the carriers of different morphology, healthy female C57Bl/6 were used for noninvasive *in vivo* SPECT imaging. The micelles were radiolabelled by encapsulating in their core an apolar complex between a chelator molecule and ^{111}In .

The results of the SPECT biodistribution show accumulation occurring primarily in liver and spleen, with partial uptake in the cortex of the kidneys. Full retention of the injected activity shows no clearance through fast pathways. While the accumulation in the kidneys is constant between the different samples, the ratio of carriers in spleen and liver changes strongly depending on the morphology of the carrier used.

The smaller spherical micelles (^{111}In -sPSS) show the longest circulation

time and a very similar uptake between liver and spleen. The larger spherical micelles, (^{111}In -sPSL), have a slightly lower accumulation in the liver when compared with the ^{111}In -sPSS, however the accumulation in the spleen shows a two fold increase. Finally the elongated micelles ^{111}In -ePSS are less uptaken by the liver but show a five fold increase in the spleen accumulation when compared with the sPSS. This is probably due to the high stiffness of the carriers which doesn't allow them to go through the spleen filtration.

All carriers show a circulation time which is longer than 24 hours, however the increase in spleen activity for the sPSL and ePSS at 48 hours suggests a higher susceptibility of the carriers to opsonisation.

CONCLUSIONS

In this work micellar carriers of different morphologies were prepared using a co-solvent evaporation method. This method allows to encapsulate hydrophobic entities in the hydrophobic core of a water soluble micelle. This technique was used to encapsulate both a hydrophobic dye by dissolving it in the organic solvent-co-polymer solution, and also to encapsulate an apolar complex formed in the aqueous phase.

The fluorescently labelled nanoparticles were used to follow their internalization in HeLa cells and the radiolabelled ones were used to determine the biodistribution of the carriers in healthy mice.

REFERENCES

- Fang, J., Nakamura, H. & Maeda, H. The EPR effect: Unique features of tumor blood vessels for drug delivery, factors involved, and limitations and augmentation of the effect. *Adv. Drug Deliv. Rev.* 63, 136–151 (2011).

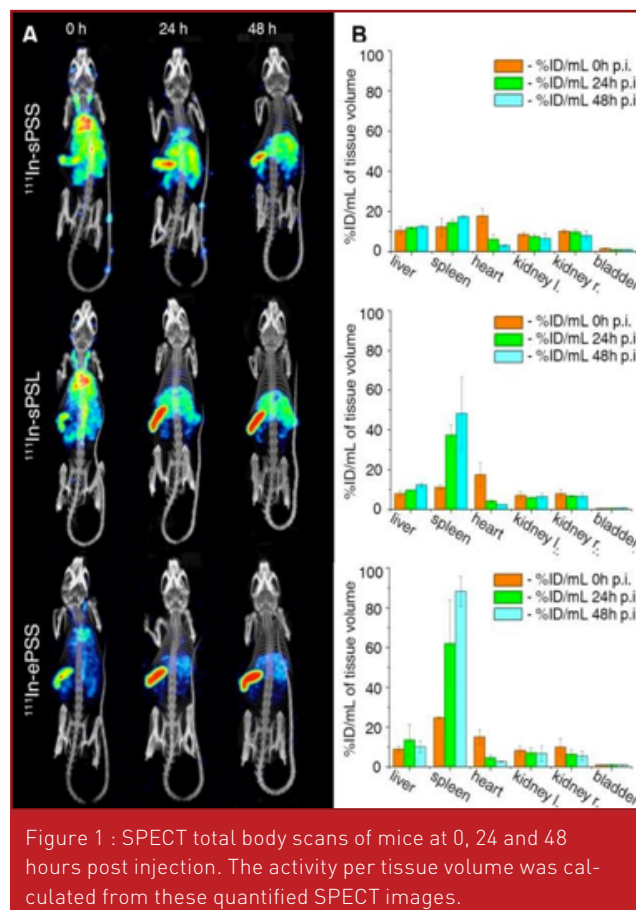


Figure 1 : SPECT total body scans of mice at 0, 24 and 48 hours post injection. The activity per tissue volume was calculated from these quantified SPECT images.

- Zhu, J. & Hayward, R. C. Spontaneous generation of amphiphilic block copolymer micelles with multiple morphologies through interfacial instabilities. *J. Am. Chem. Soc.* 130, 7496–7502 (2008).
- Cox, J. K., Yu, K., Constantine, B., Eisenberg, A. & Lennox, R. B. Polystyrene-poly(ethylene oxide) diblock copolymers form well-defined surface aggregates at the air/water interface. *Langmuir* 15, 7714–7718 (1999).

ACKNOWLEDGMENTS

The research leading to these results has received funding from the People Programme (Marie Curie Actions) of the European Union's Seventh Framework Programme (FP7/2007–2013) under REA grant agreement no. PITN-GA-2012-317019

'TRACE 'n TREAT'

¹ICS, France; ²TU Delft, Netherlands; ³MILabs B.V., Netherlands

Laurence Jennings
 Institut Charles Sardon, CNRS
 Strasbourg-France
jennings.laurence@gmail.com

SONICATION-ASSISTED LAYER-BY-LAYER NANOPARTICLES OF RESVERATROL

Santos, A. C.* , Pattekari, P.‡, Veiga, F. * , Lvov, Y. ‡, Ribeiro, A. J.*

INTRODUCTION & OBJECTIVE

Resveratrol (RSV) is a polyphenol with numerous and potent reported therapeutic activities, namely antioxidant properties. However, RSV bioavailability is compromised by its low water solubility, stability and high metabolism. These properties can be improved by the encapsulation of RSV using nanodelivery systems [Santos 2011].

Layer-by-Layer (LbL) assembly is an advanced functionality technique based on the alternate adsorption of oppositely charged polyelectrolytes (PEs) upon surfaces. This approach allows the preparation of coatings with variable compositions and controllable thickness stability [Santos 2015]. In this work, it is intended to develop RSV-loaded LbL nanoparticles (RSVNP) for encapsulation and controlled delivery of RSV, with no use of intermediate washings between PEs adsorption. RSV nanocores are prepared in water by RSV nanoprecipitation in the presence of surfactants. These surfactants form a RSV-nanocore attached layer which further anchors the LbL shell, allowing for better performance of the process. Newly and detailed characterizations of the LbL shell are made using poly(allylamine hydrochloride) (PAH) as polycation and dextran sulphate (DS) as polyanion. For this, sequential PE adsorption upon RSV nanocores is carried out by the addition of the necessary amount of PEs for each layer of the LbL shell, determined by PE titration curves. PAH and DS are used as PEs with low molecular weight, regarding their high surface charge, stability, and biocompatibility [Santos 2015, Diez-Pascual 2014]. The novelty of the present work is to prepare RSVNP for oral delivery by sonication-assisted LbL without intermediate washings, and using PAH and DS as PEs.

MATERIALS & METHODS

RSV crystals powder was dissolved in acetone at 20 mg/mL, and 60 μ L of the concentrated solution was added to an aqueous solution containing 1 mg/mL

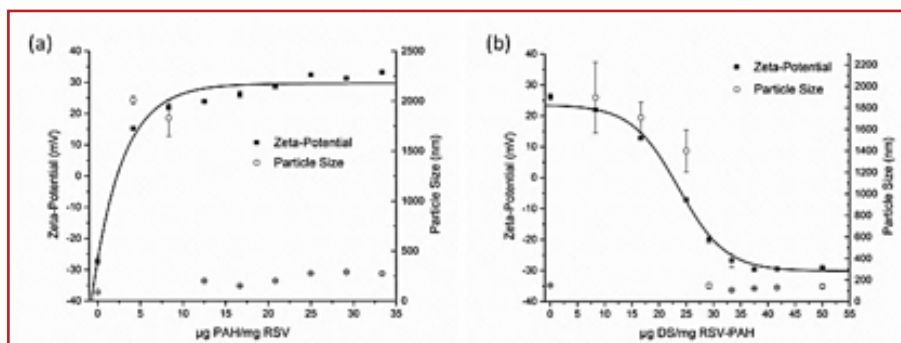


Fig. 1: PEs Titrations. Stepwise addition of [a] PAH to RSV nanocores and [b] DS to RSV-PAH NPs.

polyvinylpyrrolidone (PVP 17 PF, 7-11 kDa) and 0.005 mg/mL sodium lauryl ether sulphate (SLE2S, 28% (w/w)) at pH 3.5. Small aliquots of cationic poly(allylamine hydrochloride) (PAH, 15kDa) and anionic dextran sulphate (DS, 5 kDa) 1-4 mg/mL were added sequentially to RSV dispersion under constant sonication up to 7.5 bilayers deposition over 20-50 min. The amount of PE needed to recharge the surface of nanoparticles (NPs) was determined for each layer assembly by zeta-potential (ZP) monitoring, using electrophoretic light scattering. Particle size was monitored by dynamic light scattering. Formulations with 2.5, 5.5 and 7.5 bilayers of PEs were considered for further studies.



Encapsulation Efficiency was determined after 0.5 mL of RSVNP were added into a Centrifugal Concentrator (5 kDa MWCO) and centrifuged at 4000g for 20 min. The RSV EE was determined indirectly, after filtrate analysis by HPLC.

In vitro release kinetics of RSV from RSVNP was evaluated in HCl buffer at pH 1.2 for 2 h followed by PBS pH 6.8 up to 120 h, to simulate gastric and intestinal fluids (USPXXIV), respectively. 1 mL of RSV crystals suspension, RSV nanocores and RSV formulations were introduced into dialysis membranes devices (Float-A-Lyzer G2, 3.5 kDa MWCO)

and vertically suspended in 8 mL of release media, at 37 °C and stirred at 200 rpm. At predetermined time intervals, samples were withdrawn and replaced with equal volume of the corresponding fresh media. RSV concentration was determined by HPLC quantification.

RESULTS & DISCUSSION

RSV nanocores preparation was achieved using surfactants to prevent crystal growth and provide NPs stabilization. After nanocores preparation, for each LbL shell layer formation, the PE concentration sufficient to saturate the surface was determined by tracing PE titration curves (Fig. 1).

Intrinsic magnitude charge of initial RSV nanocores was negative, as showed in the first point of Fig. 1a, the titration of the RSV nanocores surface. Since the LbL process is based upon electrostatic interactions, RSV nanocores surface charge determined the order addition of the PEs pair. The first added PE was, thus, the polycation PAH (Fig. 1a), followed by the polyanion DS (Fig. 1b). A range of PE concentrations were investigated for each layer, regarding ZP values. In practice, the complete deposition of PE was suggested by the recharging point of each titration curve, which was the requisite to proceed for the next PE layer deposition. It can be seen in Fig. 1a that the point of plateau started at 16.7 μ g PAH/ mg RSV. In Fig. 2b, this value corresponded to 33.3 μ g DS/ mg RSV. Differences were observed between PAH and DS titrations. Upon PAH addition, an increasing effect

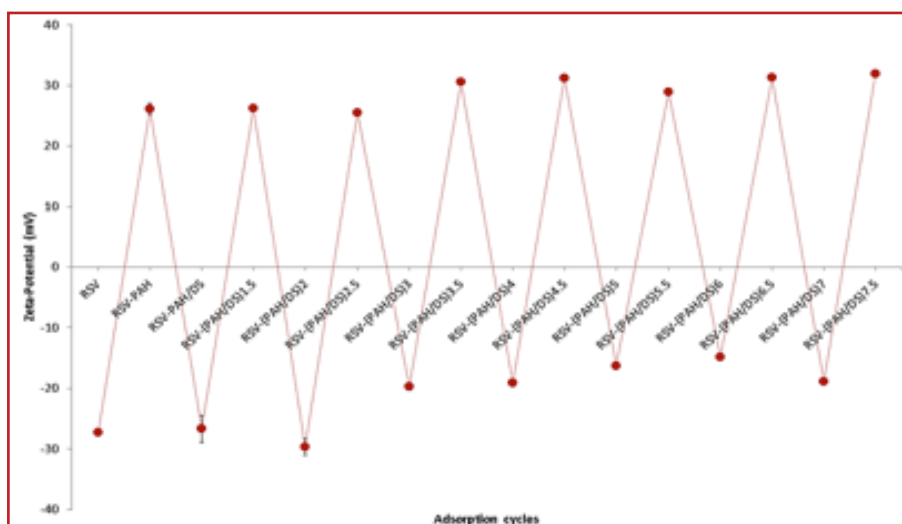


Fig. 2: ZP reversal during LbL-assembly.

on ZP value along with a more gradual plateau onset was verified, following an exponential fitting model ($R^2 > 0.96$, Fig. 1a). DS originated a clear plateau, approaching to a sigmoid fitting model ($R^2 > 0.95$, Fig. 1b). This difference could be explained to the difference in charge density of PEs. Only the two first titrations of the LbL shell were depicted, however the procedure was similar for the followed PE layers ensuring no PEs excesses. Values of ZP magnitudes during the process of adsorption are present in Fig. 2. After adsorption of PAH to RSV nanocores, drug NPs were recharged to high positive surface charge ($+26.2 \pm 1.0$ mV), conferring high physical stability to nanocores. The addition of DS promoted the reversion of the surface charge to negative values (-26.7 ± 2.2 mV). The strongly charged LbL-coated NPs repulsed, maintaining colloidal stability. The LbL proceeded by consecutively alternating PE additions. Given the higher ZP magnitude of PAH layers comparing to DS layers, PAH was chosen for the outermost shell layer coating. Thus, a LbL self-assembly technique coupled with a washless approach was developed and aqueous RSV nanocolloids with different number of PAH/DS bilayers were performed, namely with 2.5 [RSV-(PAH/DS)_{2.5}], 5.5 [RSV-(PAH/DS)_{5.5}] and 7.5 [RSV-(PAH/DS)_{7.5}] bilayers. These col-

loids showed homogenous particle size populations at the desired nanoscale interval (150-250 nm). LbL 7.5-bilayers coated NPs (the most complex formulation) showed 219 ± 1 nm and 0.17 of PI; high electrical surface ZP of $+31 \pm 0.5$ mV; and a high drug content of $92 \pm 2\%$.

In vitro release studies with RSV crystals, RSV nanocores and LbL NPs with 2.5, 5.5 and 7.5 bilayers of PAH/DS were investigated in simulated gastric followed by intestinal fluids without enzymes (Fig. 3). 2.5-bilayered coated NPs and RSV nanocores showed a higher dissolution rate in simulated gastric pH in relation to RSV crystals and 5.5 and 7.5-bilayered coated NPs. RSV crystals, in turn, showed higher dissolution rate in relation to the most complex LbL formulations. This indicates an effect of shell wall thickness on RSV delayed dissolution. Besides these differences, after 2 hours of in vitro simulated gastric incubation, most RSV remained associated to LbL NPs ($> 80\%$), indicating that these systems promoted good

gastric resistance, namely for 5.5- and 7.5-bilayered coated NPs, emphasizing the important role of LbL shell on RSV protection. Following a pH change to 6.8, a biphasic release pattern was observed, characterized by an initial rapid release during the first 1.5 hours followed by a delayed release up to 6 h. These results showed a very good fit with the exponential kinetic model ($R^2 > 0.99$), suggesting an apparent first-order behaviour. No differences were detected between 2.5-bilayered coated NPs and RSV nanocores. Both formulations led to slightly faster release than non-encapsulated RSV crystals and 5.5- and 7.5-bilayered NPs, due to the low complexity of LbL shells and also because of the NPs small size compared to micrometer size of RSV crystals (like it happened previously in simulated gastric medium). Surface area was higher between nanocores and 2.5-bilayered coated NPs and the release medium in comparison to RSV crystals. Moreover, according to Noyes-Whitney equation, an enhancement of saturation concentration and a decrease in particle size into the nanoscale caused an increase in the dissolution rate (No-khodchi 2010).

An increasing effect of the number of coating bilayers on delayed release of RSV was observed.



UNIVERSIDADE DE COIMBRA

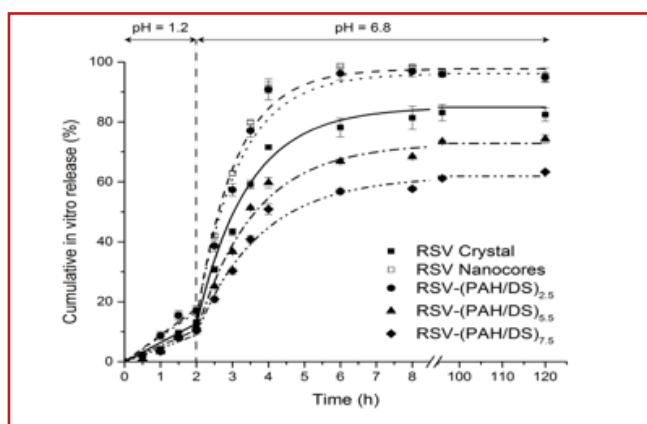


Fig. 3: In vitro RSV release from studied formulations in gastric and intestinal simulated media.

This effect was probably due to the enhancement of shell wall thickness, which conducts to increased diffusional path for RSV and, thus, for a RSV delay from the core to the LbL shell. For example, at 4 hours, only 51% of RSV in 7.5-bilayers coated NPs was released as compared with 60% the 5.5-bilayers and 91% of the 2.5-bilayers samples. Non-complete drug release from LbL PE bilayered shells was reported before and it is related to the complexity of the LbL shell. Comparing to our previous results, DS prevented significant premature release of RSV by providing higher retention capacity than polystyrenesulfonate (PSS) at gastric pH. This predicts higher availability of RSV for absorption in the intestine. Alongside, LbL technique allowed for the control of RSV release rate from PAH/DS-stabilized NPs depending on the number of coating bilayers in the

ARTICLE

shell.

CONCLUSIONS

The combination of nanocores formation by nanoprecipitation with LbL self-assembly allowed for the nanoencapsulation of RSV by using a PAH/DS-composed shell. Modification of the traditional LbL technique avoided the use of intermediate washings. We changed a traditional microencapsulation approach for well soluble drugs encapsulated in multilayer shells to a nanoarchitectural design of well dispersed low soluble RSV nanocolloids. The RSV release rate of LbL coated NPs was controlled by varying the number of PEs bilayers and shell composition. Moreover, using a PAH/DS-composed shell showed to significantly retain RSV in simulated stomach conditions, being the present technique proposed to formulate a viable oral delivery system for RSV.

REFERENCES

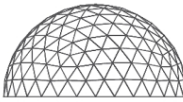
- Santos, A. C., Veiga, F. & Ribeiro, A. J. New delivery systems to improve the bioavailability of resveratrol. *Expert Opin. Drug Deliv.* 8, 973-990 (2011).
- Santos, A. C., Pattekari, P., Jesus, S. et al. Sonication-assisted layer-by-layer assembly for low soluble drug nanoformulation. *ACS Appl. Mater. Interfaces*, doi:10.1021/acsami.5b02002 (2015).
- Díez-Pascual, A. & Shuttleworth, P. Layer-by-layer assembly of biopolyelectrolytes onto thermo/pH-responsive micro/nano-gels. *Materials* 7, 7472-7512 (2014).
- Nokhodchi, A., Amire, O. & Jelvehgari, M. Physico-mechanical and dissolution behaviours of ibuprofen crystals crystallized in the presence of various additives. *Daru, J. Pharm. Sci.* 18, 74-83 (2010).

*FFUC, Portugal; ‡ Louisiana Tech Univ., USA



Ana Claudia Santos
University of Coimbra
Pharmaceutical Technology
Coimbra - Portugal
ana.cl.santos@gmail.com

CALENDAR

PROGRAM 2016	
February	 <p>9th International Conference on Advanced Technologies & Treatments for Diabetes (ATTD 2016) February 3-6, 2016 Milan, Italy http://www.attd2016.com/</p>
March	 <p>11th biennial Conference and Workshop on Biological Barriers March 7-9, 2016 Saarland Gerlmany https://www.kwt-uni-saarland.de/en/booking/bio-barriers-englisch/conference-program.html</p>
April	<p>PBP WORLDMEETING</p> <p>10th World Meeting on Pharmaceutics, Biopharmaceutics and Pharmaceutical Technology April 4-7, 2016 Glasgow, UK http://www.worldmeeting.org/home/</p>  <p>19th Microencapsulation Industrial Convention April 4-6, 2016 Frankfurt, Germany http://bioencapsulation.net/2016_Frankfurt</p>  <p>Design and Manufacture of Functional Microcapsules and Engineered Particles April 3-8, 2016 Siracusa (Sicily), Italy http://www.engconf.org/conferences/materials-science-including-nanotechnology/</p>
May	 <p>10th World Biomaterials Congress Injectable biomaterials for cell therapy and tissue engineering May 17-22, 2016 Montreal, Canada WBC2016.org</p>
May - June	 <p>8th Training School on Microencapsulation May 30 - June 2, 2016 Cork, Ireland http://bioencapsulation.net/2016_Cork</p>  <p>NANO IN BIO 2016, May 31- June 5, 2016, Le Gosier (Guadeloupe, FWI) (France) http://nanoinbio2016.sciencesconf.org</p>
June	 <p>International Symposium on Polyelectrolytes 2016 June 27-30, 2016 Moscow, Russia www.isp2016.org</p>
August	 <p>24th International Congress of Theoretical and Applied Mechanics August 21-26, 2016 Montréal, Canada www.ictam2016.org</p>

USE OF VEGETABLE OILS ON FORMULATION OF EFFICIENT BIOACTIVE LIPID NANOCARRIERS

Pinto, F., De Barros, D.P.C., Fonseca, L.P. – Instituto Superior Técnico, Universidade de Lisboa, Portugal

INTRODUCTION AND OBJECTIVES

The use of natural ingredients is highly pursued, particularly in cosmetics, with an ongoing search for developing efficient products with broad biological relevance (Niculae et al., 2013). Vegetable or natural oils exhibit great interest as raw materials in all sectors of industry, due to their well-known beneficial health effects. They present inherent antioxidant, anti-carcinogenic and anti-inflammatory activities which are maintained or can be enhanced once encapsulated at nanoscale (Badea et al., 2015). Solid lipid nanoparticles (SLNs), nanostructured lipid carriers (NLCs), nanoemulsions (NEs) and nanocapsules (NCs), have been used to incorporate and deliver active molecules in cosmetic products (Montenegro, 2014). NLCs are composed of a mixture of solid lipids and oils that is stabilized by an outer layer of surfactants and which allows the formation of an overall amorphous nanostructured with many imperfections within its matrix, providing NLCs a higher drug capacity and a lesser degree of drug expulsion during storage (Zheng et al., 2013). These lipid systems are safe and biodegradable carriers due to their generally recognized as safe (GRAS) ingredients. Moreover, the NLCs present several advantages as improved drug loading capacity and less drug expulsion during storage, enhanced permeation, low production

cost and are easy to scale up (Pinto et al., 2014).

The main subject under scope of this work is to develop safe and effective lipid nanocarriers based on natural ingredients that can be incorporated in cosmetic formulations to successfully deliver active ingredients. The present study aimed to evaluate the influence of vegetable oils in different proportions and the effect of the fatty acid chain length of solid lipids on structure and on physicochemical properties of NLCs. Contributions of the solid and liquid lipids to the particle distribution were analyzed by dynamic light scattering (DLS).

MATERIALS & METHODS

Materials

Solid lipids: capric acid, C10 ($\geq 98\%$); lauric acid, C12 ($\geq 98\%$); myristic acid, C14 (Sigma Grade, $\geq 99\%$); palmitic acid, C16 ($\geq 99\%$) and stearic acid, C18 ($\geq 95\%$) were purchased from Sigma-Aldrich (St. Louis, MO, USA). Liquid oils: Sunflower oil (SF), (Fula, Portugal) and olive oil (OV), (Gallo, Portugal) were food grade commercial products; sweet almond oil (SA), (Well's, Portugal) cosmetic grade; coconut oil (CO), with analytical grade (Supelco, USA). Tween 80 (polyoxyethylene sorbitan monooleate) was obtained from Merck (Darmstadt, Germany). The aqueous phase of miniemulsions was prepared with Milli-Q water.

Preparation of NLCs

The vegetable oil-NLCs were prepared by the miniemulsions methodology with an ultrasonication step. The aqueous phase consisted in 2,5% (wt%) of surfactant (Tween 80) in Milli-Q water and the lipid phase, 5% (wt%), consisted in a

blend of a solid lipid with a vegetable oil. The lipid phase was heated to 70°C until the solid and liquid lipids were blended and melted to form a uniform and clear oil phase. This phase was after added to the aqueous at the same temperature and both phases were mixed by the aid of magnetic stirring for 30 min. The pre-miniemulsion was then fully homogenized with a probe-type sonicator (Sonopuls - Ultrasonic homogenizer, Bandelin, Germany) for 5 min. The resultant nanoemulsion was subsequently cooled to room temperature and stored.



Characterization of particle size, PDI and surface charge

Particle size, which yields the hydrodynamic diameter, R_d (intensity weighted mean diameter) and polydispersity index (PDI) were determined by dynamic light scattering (DLS), using a Malvern Zetasizer Nano ZS (Malvern Instruments, UK). Prior to measurements, all samples were diluted using Milli-Q water to produce an adequate scattering intensity. All measurements were performed at 25°C and data was given as average of three individual measurements. Each measurement was performed in triplicate at 25°C. The zeta potential (ZP) reflects the electric charge on the particle surface and indicates the physical stability of colloidal systems and it was measured with the same equipment by using electrophoretic light scattering technique.

RESULTS & DISCUSSION

Effect of oil content and composition on NLCs size and physical stability

In this study, NLCs were prepared with capric acid (C10) as solid lipid and with

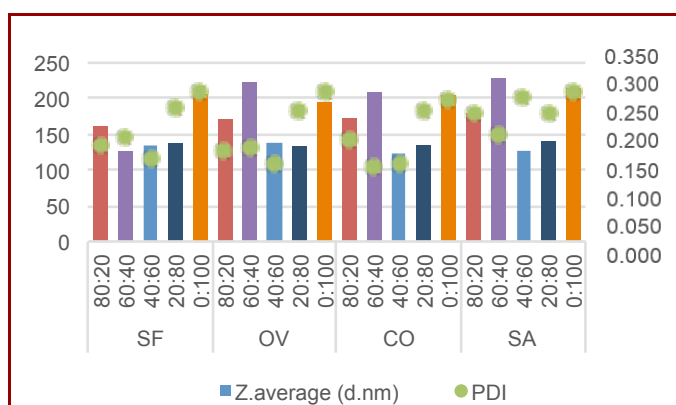


Figure 1 – Mean particle size and PDI data of NLC formulations based on particle size measurements. Influence of oil content and composition on NLCs made from capric acid (C10) as solid lipid.

ARTICLE

different vegetable oils. The percentage of lipid phase (blend of solid lipid and liquid oil) on the miniemulsions was kept constant being 5% (w/w) of the total formulation, while the liquid oil content in the lipid phase was varied in to different solid lipid to oil ratios.

The mean particle size (Z.average), the polydispersity index and zeta potential of the lipid nanocarriers are illustrated in Figures 1 and 2, respectively. NLCs with particle sizes ranging from 126 to 228 nm and with relatively uniform particle size distributions (PDI of 0.145 - 0.293) were obtained. It could be observed in Figure 1, that the average size of the NLC decreases with the increase of liquid oil amount up to 80%. This may be due to that the liquid oil could be more easily dispersed into the aqueous phase and contributed to smaller particles (Zheng et al. 2013). On the other hand, the difference on the fatty acid compositions of the used vegetable oils seems to have low influence on the particle size of final NLCs being this affected by the percentage of oil on the lipid matrix. The lowest average sizes were obtained with 40:60 and 20:80 ratios, independently of the used oil, with an exception for the 60:40 [capric acid: sunflower oil] ratio which also demonstrated a low value.

The physical stability of colloidal systems is determined in function of zeta potential, which quantifies the particle charge. In theory, higher values of zeta potential, either positive or negative, end to stabilize the suspension and aggregation phenomena are less likely to occur for charged particles with

pronounced zeta potential ($>|30|$), due to the electrostatic repulsion between particles with the same electrical charge (Pinto et al. 2014) The determined zeta potential values of the formulated NLCs ranged between -17.1 and -23.0 mV (Figure 2), which predicts a short-term stability to the particles.



TÉCNICO LISBOA

Effect of fatty acid chain length of the solid lipid on NLCs size and surface charge

From the previous study it was chosen the more suitable percentage of vegetable oil on the lipid phase, that corresponds to the 40:60 ratio, and it was kept constant. The NLCs were prepared with saturated solid fatty acids ranging from C10 to C18, in order to study the effect of the chain length on particle size and physical stability

The particle sizes and PDI of the NLCs, assessed by DLS, are presented in Figure 3. It can be observed that increasing the length of the solid fatty acid demonstrated to have low influence on NLCs size.

All the formulations with the different vegetable oils had little variations on particle size with the increase of the chain length of the solid lipid. Despite that, lipid nanocarriers made from

sunflower oil had the lowest particle sizes which decrease with the increase of the solid fat chain length (136 nm with C10 and 76 nm with C18). This could be due to a higher proportion of linoleic acid, an unsaturated lipid, on sunflower oil composition when compared with the other oils. The polydispersity parameter, gives an important information concerning on sample homogeneity (Pinto et al. 2014). The obtained PDI values were below 0.290, which reflects relatively homogeneous nanoparticles. Regarding the physical stability of the obtained lipid nanocarriers, it was found that the increase in the fatty acid chain length had the same low effect that was noticed with the particles size. The zeta potential values were above -22.0 mV for all the NLCs formulations with the different vegetable oils, indicating a short-term stability to the particles and that this parameter needs to be improved.

CONCLUSION

Through this work, it could be concluded that all formulations led to the development of suitable NLCs, presenting characteristics that would render them as promising nanocarriers with high incorporation potential of active ingredients. Lipid nanocarriers with particle sizes ranging from 76 to 228 nm and with a narrow particle size distribution were obtained by the miniemulsion methodology. The percentage of vegetable oil in the lipids phase of the miniemulsions demonstrated to have influence on particle size of NLCs. In a contrary way, the differences on the fatty acids composition of the vegetable oils and the fatty acid chain length of solid lipids had a low impact in both size and surface charge of the obtained lipid nanocarriers. Negative zeta potential values above -23.0 were determined, which characterizes the particles with a short-term physical stability, being

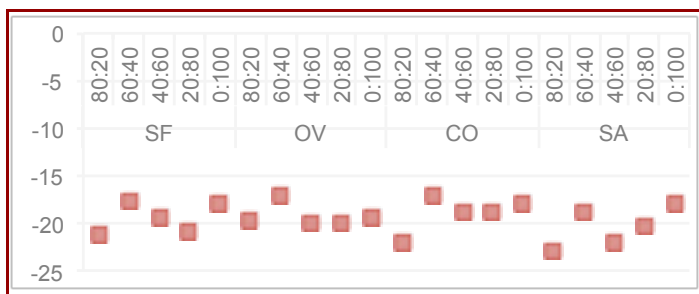


Figure 2 – Zeta potential values of NLCs synthesized with different vegetable oils and solid lipid to oil ratios

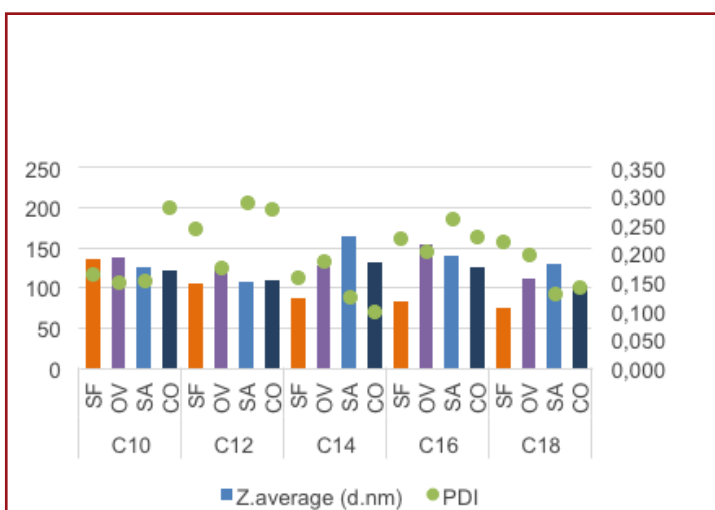


Figure 3 – Z.average and PDI data based on particle size measurements. Influence of fatty acid chain length of the solid lipid on NLCs size, with a constant oil percentage (40:60, solid lipid: vegetable oil).

ARTICLE

necessary to improve this parameter. Further analysis of melting behavior, crystalline state and rheological behavior of the particles are necessary for the full physicochemical characterization of NLCs. Finally, the potential of these lipid particles as safe and efficient nanocarriers, to be used on cosmetic formulations, is being evaluated by the determination of the entrapment efficiency to different active ingredients with commercial interest.

REFERENCES

- Badea G., Lacatus I., Badea N., et al. Use of various vegetable oils in designing photoprotective nanostructured formulations for UV protection and antioxidant activity. *Industrial Crops and Products*. 67, 18–24 (2015)
- Montenegro L. Nanocarriers for skin delivery of cosmetic antioxidants. *Journal of Pharmacy & Pharmacognosy Research*, 2 (4), 73–92 (2014)
- Niculae G., Lacatus I., Badea N., et al. Influence of vegetable oil on the synthesis of bioactive nanocarriers with broad spectrum photoprotection. *Cent. Eur. J. Chem.* 12 (8), 837–850 (2013)
- Pinto, M.F., Moura, C.C., Nunes, C., et al. A new topical formulation for psoriasis: Development of 3 methotrexate-loaded nanostructured lipid carriers. *International Journal of Pharmaceutics*. 477, (1–2), 519 – 526 (2014)
- Zheng M., Falkeborg M., Zheng Y., et al. Formulation and characterization of nanostructured lipid carriers containing a mixed lipids core. *Colloids and Surfaces A: Physicochem. Eng. Aspects* 430, 76– 84 (2013)



Fatima Pinto

Instituto Superior Tecnico Lisbon
Bioengineering
Lisbon - Portugal
fatima.pinto@tecnico.ulisboa.pt

BIBLIOGRAPHY



Journal of Microencapsulation Vol. 32, Number 7 (2015)

<http://www.tandfonline.com/toc/imnc20/32/7>

- **Exploitation of pleiotropic actions of statins by using tumour-targeted delivery systems**
Emilia Licarete, Alina Sesarman & Manuela Banciu
pages 619–631
- **Enhanced stability of oral insulin in targeted peptide ligand trimethyl chitosan nanoparticles against trypsin**
Jiexiu Chen, Chong Liu, Wei Shan, Zhijian Xiao, Han Guo & Yuan Huang
pages 632–641
- **Synthesis of microcapsules containing different extractant agents**
Ángela Alcázar, Manuel Carmona, Ana M. Borreguero, Antonio de Lucas & Juan F. Rodríguez
pages 642–649
- **Cotton fabric functionalisation with menthol/PCL micro- and nanocapsules for comfort improvement**
Raffaella Mossotti, Ada Ferri, Riccardo Innocenti, Tereza Zelenková, Francesca Dotti, Daniele L. Marchisio & Antonello A. Barresi
pages 650–660
- **Inhalable, large porous PLGA microparticles loaded with paclitaxel: preparation, in vitro and in vivo characterization**
Shohreh Alipour, Hashem Montaseri & Mohsen Tafaghodi
pages 661–668
- **Study on the effects of microencapsulated *Lactobacillus delbrueckii* on the mouse intestinal flora**
Qingshen Sun, Yue Shi, Fuying Wang, Dequan Han, Hong Lei, Yao Zhao & Quan Sun
pages 669–676
- **Optimization of paeonol-loaded microparticle formulation by response surface methodology**
Sha-Sha Li, Guo-Feng Li, Li Liu, Hui Li, Xiao Jiang, Xue-Ling Li, Zhi-Gang Liu, Ting Zuo, Li-Dong Weng & Qiang Liu
pages 677–686
- **ICAM-1 targeted catalase encapsulated PLGA-b-PEG nanoparticles against vascular oxidative stress**
Ece Sari, Yeliz Tunc-Sarisozen, Huyla Mutlu, Reza Shahbazi, Gulberk Ucar & Kezban Ulubayram
pages 687–698
- **Preparation and cellular targeting study of VEGF-conjugated PLGA nanoparticles**
Yaling Shi, Mingyao Zhou, Jie Zhang & Wen Lu
pages 699–704
- **Fabrication of redox-responsive magnetic protein microcapsules from hen egg white by the sonochemical method**
Shuangling Zhong, Xuejun Cui & Fangyuan Tian
pages 705–710
- **Preparation, release and physicochemical characterisation of ethyl butyrate and hexanal inclusion complexes with β - and γ -cyclodextrin**
Yang Zhang, Yibin Zhou, Shengnan Cao, Songnan Li, Shanshan Jin & Shu Zhang
pages 711–718
- **Effect of emulsification and spray-drying microencapsulation on the antilisterial activity of transcinamaldehyde**
Nga-Thi-Thanh Trinh, Raja Lejmi, Adem Gharsallaoui, Emilie Dumas, Pascal Degraeve, Mai Le Thanh & Nadia Oulahal
pages 719–723

Vol. 32, Number 8 (2015)

<http://www.tandfonline.com/toc/imnc20/32/8>

- **Spray congealing as a microencapsulation technique to develop modified-release ibuprofen solid lipid microparticles: the effect of matrix type, polymeric additives and drug-matrix miscibility**
Priscilla Chui Hong Wong, Paul Wan Sia Heng & Lai Wah Chan
pages 725–736
- **Preparation, characterisation and thermal properties of calcium alginate/n-nonadecane microcapsules fabricated by electro-coextrusion for thermo-regulating textiles**
Meghdad Kamali Moghaddam & Sayed Majid Mortazavi
pages 737–744
- **Drug-carrier interaction analysis in the cell penetrating peptide-modified liposomes for doxorubicin loading**
Chang Liu, Qi Luo, YingFeng Tu, Gui-Ling Wang, YingChun Liu & Ying Xie

BIBLIOGRAPHY

pages 745-754

- **Development of chitosan-pullulan composite nanoparticles for nasal delivery of vaccines: optimisation and cellular studies**
Erdal Cevher, Stefan K. Salomon, Apostolos Makrakis, Xiong Wei Li, Steve Brocchini & H. Oya Alpar
pages 755-768
- **Development of chitosan-pullulan composite nanoparticles for nasal delivery of vaccines: in vivo studies**
Erdal Cevher, Stefan K. Salomon, Satyanarayana Somavarapu, Steve Brocchini & H. Oya Alpar
pages 769-783
- **SN-38 active loading in poly(lactico-glycolic acid) nanoparticles and assessment of their anticancer properties on COLO-205 human colon adenocarcinoma cells**
Sherief Essa, Jamal Daoud, Michel Lafleur, Sylvain Martel & Maryam Tabrizian
pages 784-793
- **A pH-triggered delayed-release chronotherapeutic drug delivery system of aceclofenac for effective management of early morning symptoms of rheumatoid arthritis**
Krishna Sanka, Rajeswara Rao Pragada & Prabhakar Reddy Veerareddy
pages 794-803
- **Evaluation of antibacterial activity of caffeic acid encapsulated by β -cyclodextrins**
Eva Pinho, Graça Soares & Mariana Henriques
pages 804-810
- **Preparation and detection of calcium alginate/bone powder hybrid microbeads for in vitro culture of ADSCs**
Kedong Song, Xinyu Yan, Shixiao Li, Yu Zhang, Hong Wang, Ling Wang, Mayasari Lim & Tianqing Liu
pages 811-819
- **Lyophilised Vegetal BM 297 ATO-Inulin lipid-based synbiotic micro-particles containing *Bifidobacterium longum* LMG 13197: design and characterisation**
A. C. Amakiri, L. Kalombo & M. S. Thantsha
pages 820-827

Artificial Cells, Nanomedicine and Biotechnology Vol. 43, Number 5 (2015)

<http://www.tandfonline.com/toc/ianb20/43/5>

- **Stimuli-sensitive Systems-an emerging delivery system for drugs**
Ankur Bhardwaj, Lalit Kumar, Shuchi Mehta & Abhinav Mehta
pages 299-310
- **Biogenic gold nanoparticles: As a potential candidate for brain tumor directed drug delivery**
R. M. Tripathi, Archana Shrivastav & B. R. Shrivastav
pages 311-317
- **Fibronectin-Alginate microcapsules improve cell viability and protein secretion of encapsulated Factor IX-engineered human mesenchymal stromal cells**
Bahareh Sayyar, Megan Dodd, Leah Marquez-Curtis, Anna Janowska-Wieczorek & Gonzalo Hortelano
pages 318-327
- **Bilayer mucoadhesive microparticles for the delivery of metoprolol succinate: Formulation and evaluation**
Krishan Kumar, Neha Dhawan, Harshita Sharma, Pramod S. Patwal, Shubha Vaidya & Bhuvaneshwar Vaidya
pages 328-333
- **Development and characterization of nanoemulsion as carrier for the enhancement of bioavailability of artemether**
Moksha Laxmi, Ankur Bhardwaj, Shuchi Mehta & Abhinav Mehta
pages 334-344
- **Preparation and characterization of PEG-modified PCL nanoparticles for oxygen carrier: a new application of Fourier transform infrared spectroscopy for quantitative analysis of the hemoglobin in nanoparticles**
Xiaoqian Shan, Yuan Yuan & Changsheng Liu
pages 345-354
- **Nodavirus-based biological container for targeted delivery system**
Pitchanee Jariyapong
pages 355-360

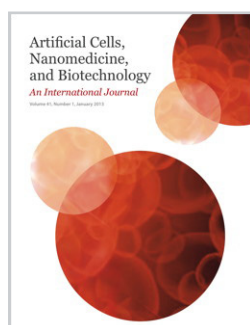
Vol. 43, Number 6 (2015)

<http://www.tandfonline.com/toc/ianb20/43/6>

- **Study on clinical application of nano-hydroxyapatite bone in bone defect repair**

Weimin Zhu, Daping Wang, Jianyi Xiong, Jianquan Liu, Wei You, Jianghong Huang, Li Duan, Jieli Chen & Yanjun Zeng
pages 361-365

- **Chitosan nanoparticles as a potential nonviral gene delivery for HPV-16 E7 into mammalian cells**
Alireza Tahamtan, Alijan Tabarraei, Abdolvahab Moradi, Meshkat Dinarvand, Mishar Kelishadi, Amir Ghaemi & Fatemeh Atyabi
pages 366-372
- **Ex vivo localization and permeation of cisplatin from novel topical formulations through excised pig, goat, and mice skin and in vitro characterization for effective management of skin-cited malignancies**
Vandana Gupta & Piyush Trivedi
pages 373-382
- **Effect of active Notch signaling system on the early repair of rat sciatic nerve injury**
Jin Wang, Ke-Yu Ren, Yan-Hua Wang, Yu-Hui Kou, Pei-Xun Zhang, Jian-Ping Peng, Lei Deng, Hong-Bo Zhang & Bao-Guo Jiang
pages 383-389
- **Simulation and verification of macroscopic isotropy of hollow alginate-based microfibers**
Sabra Djomehri, Hanaa Zeid, Alireza Yavari, Maryam Mobeid-Miremadi, Kenneth Youssefi & Sindy Liao-Chan
pages 390-397
- **Hematopoietic repopulating ability of CD34+ progenitor cells ex vivo expanded with different cytokine combinations**
Zheng Du, Huili Jin, Haibo Cai, Shi Yang & Wen-song Tan
pages 398-402
- **Heparin removal from human plasma using molecular imprinted cryogels**
Gözde Baydemir & Adil Denizli
pages 403-412
- **Sonication-assisted drug encapsulation in layer-by-layer self-assembled gelatin-poly(styrene-sulfonate) polyelectrolyte nanocapsules: process optimization**
Abhijeet P. Pandey, Saurabh S. Singh, Ganesh B. Patil, Pravin O. Patil, Chetan J. Bhavsar & Prashant K. Deshmukh
pages 413-424
- **Characterization and immobilization of *Trametes versicolor* laccase on magnetic chitosan-clay composite beads for phenol removal**
Tülin Aydemir & Semra Güler
pages 425-432



THESES ABSTRACTS



Structuring and control of physicochemical properties of alginate liquid-core capsules by biopolymers association

GHAZI BEN MESSAOUD

Supervisor Stéphane Desobry; Laura Sanchez
Date & Place 29-10-2015 – Nancy, France
Affiliation Lorraine University, France

The aim of this thesis is to study the physicochemical properties of alginate liquid-core capsules and to control their permeability and mechanical properties by biopolymers blending. These millimeter-scale size capsules are prepared by a reverse spherification process. In a first work, the influence of polymers used to control capsule liquid-core viscosity (thickening agent) during capsules preparation on permeability and mechanical stability of the alginate membrane was investigated. The mechanical properties of capsules were correlated with viscoelastic properties of plane alginate hydrogels characterized by small amplitude oscillatory shear rheology. In a second work, composite capsules with a membrane of sodium caseinate / alginate were developed and showed improved stability and pH-dependent release of a dye used as a model molecule. Finally, the influence of shellac incorporation in alginate membrane or as an external coating layer resulted in enhanced properties and decreased membrane permeability against low molecular weight molecules. Alginate capsules have a wide range of applications which requires a better understanding and control of their properties.

ghazi.benmessaoud@hotmail.fr



Encapsulation of nisin-producer *Lactococcus lactis* strain, for active packaging development

MARIAM FLEAR AZIZ BEKHIT

Supervisor Stéphane Desobry
Date & Place 30-10-2015 – Nancy, France
Affiliation Université de Lorraine, France

The present PhD work aimed to design biopolymeric active packaging entrapping bioprotective lactic acid bacteria (LAB) and control undesirable microorganisms growth in foods, particularly *L. monocytogenes*. First, the mechanical and chemical stability of the alginate beads were improved, and consequently the effectiveness of encapsulation was increased. Alginate/pectin (A/P) biopolymers were prepared, as first microspheres design, by extrusion technique to encapsulate nisin-producing *Lactococcus lactis* subsp. *lactis* in different physiological state (exponential phase, stationary phase). Results showed that A/P composite beads were more efficient to increase beads properties than those formulated with pure alginate or pectin. Association of alginate and pectin induced a synergistic effect which improved microbeads mechanical properties. As a second microspheres design, aqueous-core microcapsules were prepared with an alginate hydrogel membrane and a xanthan gum core. Results showed that microcapsules with *L.lactis* in exponential state gave the best results and exhibit interesting antilisterial activity. These microparticles were applied in food preservation and particularly in active food packaging. A novel bioactive film (HPMC, starch) was developed and tested, entrapping active beads of alginate/xanthan gum core-shell microcapsules and alginate/pectin hydrogel enriched with *L.lactis*.

mariam.bekhit@univ.lorraine.fr, mariamflear@yahoo.com



β -lactoglobulin and lactoferrin complex coacervates: characterization and putative applications as encapsulation device

GUILHERME TAVARES

Supervisor Saïd Bouhallab
Date & Place 08-10-2015 – Rennes, France
Affiliation INRA/STLO, France & UFV, Brazil

Recent studies showed the ability of oppositely charged food proteins to co-assemble into microspheres through complex coacervation. Understanding the driving forces governing heteroprotein coacervation process and how it is affected by bioactives is a prerequisite to use heteroprotein coacervates as encapsulation device. The conditions of optimal β -LG - LF coacervation were determined as well as the constituent molecular species of the coacervate phase. To evaluate the β -LG - LF complex coacervation in the presence of small ligands, models of hydrophobic (ANS) and hydrophilic molecules (folic acid) were used. High relative concentrations of small ligands led to a transition from coacervation to aggregation regime.

gtavares@agrocampus-ouest.fr



Investigation of Particle Movement in a Lab-Scale Spray Coater

EMRE KARAOĞLAN

Supervisor Denis Poncelet; Olivier Rouaux; Sébastien Curet-Ploquin
Date & Place 26-10-2015 – Nantes, France
Affiliation ONIRIS, France

The objective of this work is to develop an understanding of particle motion in a lab scale spray coater in terms of various operating conditions, material properties and reactor design. The airflow rate and its distribution passing through the reactor was quantified using hot-wire anemometry. The experimental data was used to construct a standard $k-\epsilon$ turbulent flow model to predict airflow in the reactor. Particle movement in the reactor was measured with respect to airflow rate, particle size, reactor load and reactor interior design using positron emission particle tracking. Particle circulation time distributions, time-averaged solid concentration over the reactor, radial/axial particle velocity profiles and zone-wise particle residence within the reactor were calculated using the post-processing program, developed to analyze PEPT data. Shorter and narrowly distributed particle circulations were observed when the airflow was increased. A similar behavior was observed when the particle load in the reactor was increased or the particle size was decreased. Introduction of a spouting apparatus at the bottom of the reactor significantly changed the circulation trajectory of the particles, resulting in faster and narrowly distributed particle circulation times. Using the airflow model and the experimental data obtained, a gas-solid fluidization model was constructed. The particle flow was modeled in a discrete description of motion over a finite element discretized domain for the first time in the literature. The model was able to qualitatively predict particle motion, despite lacking quantitative accuracy.

ekaraoglan@yahoo.com.tr

PRODUCTION OF CAPSULES BY COEXTRUSION FOR COLON DELIVERY

Bidoret A¹, Binti Mohd Saleh NS¹, Acevedo F², Morales E², Guéraud F³, M. Penning⁴, Poncelet D¹

INTRODUCTION & OBJECTIVE

Co-extrusion of an oil phase in a gel forming phase in a form of a jet, breaking the jet in droplets under vibration and collecting the droplets in a gelification bath results in core-shell capsules. The technology appears quite versatile but has been mainly applied only for alginate shell (Whelehan & Marison, 2009).

The objective of this work is to combine alginate with other polymers to form microcapsules able to deliver actives, such drug, in intestine and more specifically in colon.



MATERIALS & METHODS

Alginate (Algogel 3001) was kindly provided by Cargill, France; shellac (Norevo B20, 250 g/L) by Norevo, Germany; eudragit (FS 30 D, 300 g/L) by Evonik. Sunflower oil was supplied by Scamark France. Other components were purchased from usual chemical suppliers.

Alginate solutions were produced by sprinkling alginate powder onto equal volume distilled water solution under high mixing followed by one-hour de-aeration. Alginate/shellac or alginate/

eudragit solutions were obtained by mixing in different proportions alginate solution and shellac or eudragit solution and pH adjusted to 7. Composition will be referred in the text as final concentration in g/L. Oil phase was composed of sunflower oil added of 0,1 % Sudan red as colorant.

Microcapsules were produced using an Encapsulator B390 (Buchi, Switzerland), equipped with a double co-extrusion head (Figure 1). Oil phase was fed to the internal nozzle using a syringe pump while shell solution was supplied to the external nozzle using under pressure vessel. Droplets were dropped in a CaCl₂ solution (15 g/L) adjusted at pH 5. Capsules are hardened for 5 minutes, then filtered, washed with distilled water and dried on absorbent paper for 24 hours.

Capsules were observed by optic microscope for the morphology and size. Capsule swelling was realized by introducing ≈ 1 g of capsules (M0) in a tea bag, submerged in phosphate buffers at different pH for 3 hours, and swollen capsule mass recorded (Mf). Swelling factor was defined as :

$$f = M_f / M_0 \quad (1)$$

Haake 550 viscosimeter (Thermo-Electron, USA) was used at constant temperature (25 °C) to measure the viscosity of the different solutions.

RESULTS

Production of alginate capsules

For alginate concentration equal or lower than 10 g/L, irregular and multicore capsules were formed. Concentrations equal or higher than 30 g/L result in too viscous solution and jet breakage was not stable. For 15 and 20 g/L concentration spherical microcapsules

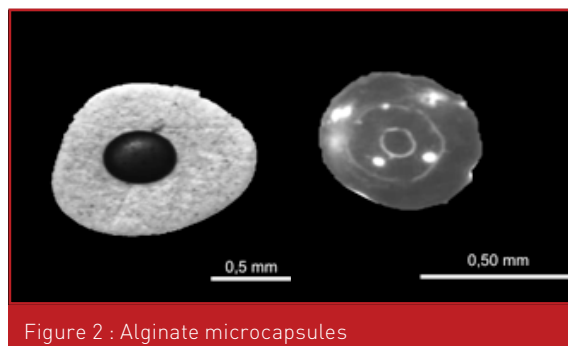


Figure 2 : Alginate microcapsules

with single core were formed with a wet capsule diameter of 1.7 to 1.9 mm and dry capsule diameter of 0,7 mm.

A series of Light-Emitting Diodes (LED) placed on back of the jet and flashing at the same frequency than the nozzle vibration. If the breakage is optimum, the drops seem motionless in front of the LEDs. The frequency of the nozzle vibration was varied from 50 to 450 Hz with an optimum at 250 Hz. The effect of the oil internal flow and internal nozzle diameter was also evaluated to conclude that 0.5 mL/min flow and nozzle diameter of 200 or 300 μ m provided the lower microcapsule size dispersion and more spherical capsules. Optimum conditions to produce correct alginate microcapsules were then defined as (Figure 2):

- External and internal flows of 11-15 and 0.5 mL/min
- External and internal nozzles of 500 and 300 μ m
- Vibration frequency and amplitude of 250 Hz and 2
- Dispersive voltage 2000 V.

Tests in vivo done in INRA Toxalin group (Toulouse) showed that alginate capsules break even before to reach the intestine. However, alginate provides exceptional gelification properties. Enteric polymers (shellac or eudragit) were added to the alginate to improve the microcapsule properties.

Production of alginate/shellac microcapsules

Shellac solution (250 g/L) was mixed with alginate solution (20 g/L) in dif-



Figure 1 : Encapsulator B390 & co-extrusion

ARTICLE

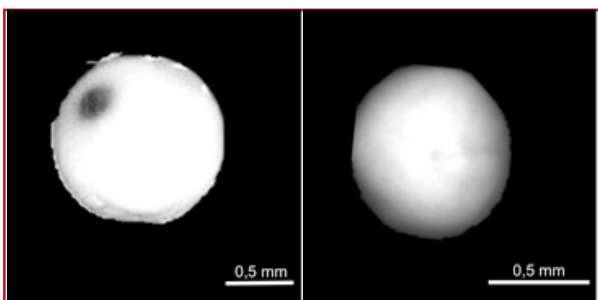


Figure 3 : alginate/ shellac (10/125 g/L) microcapsules

ferent proportions. The mixtures were not stable and phase separation occurred, even while pH was adjusted to 7 as recommended by the Shellac supplier. The mixtures were then treated with a high shear mixer (Ultraturax IKA25) for 5 minutes before producing the capsules. In case of alginate/shellac, CaCl_2 solution was prepared using V/V water/ethanol solution to promote shellac precipitation.

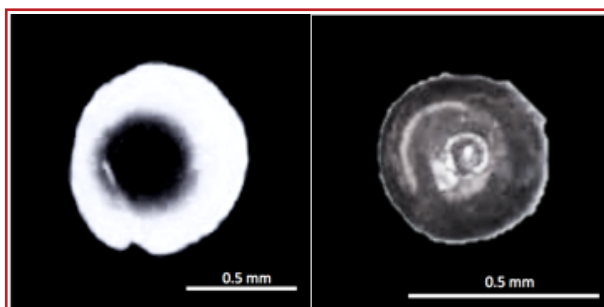


Figure 4 : alginate/eudragit (15/9 g/L) microcapsules

Relatively spherical and mono-core capsules were obtained for final shellac concentration between 125 to 180 g/L (Figure 3), showing very little agglomeration. Higher shellac concentration results in irregular capsules, probably due to too low viscosity of the solution (18 ± 2 mPa.s) causing deformation while penetrating the gelation bath.

Spherical and mono-core capsules were obtained for internal nozzle diameter ranging from 80 to 300 but

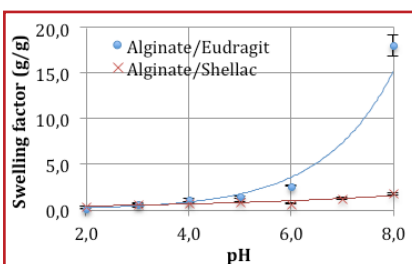


Figure 5 : Swelling of the microcapsules versus pH

only while external-to-internal diameter ratios higher than 1.6. For lower ratio, agglomeration and oil release occurred.

Production of alginate/eudragit microcapsules

Eudragit FS30D is provided as a nano-sized suspension with an acidic pH. Despite the size of the particles, some nozzle blockings were observed. Eudragit particles dissolve when pH is rising but leading to very viscous solution. The mix alginate (15 g/L) et eudragit (300 g/L) was filtered. Up to 60 g/L of eudragit final concentration leads to relatively spherical and mono-core capsules (Figure 4).

Swelling of microcapsules

To test in vitro the behavior of the capsules during the gastro-intestinal tracts, microcapsules were introduced into different pH phosphate buffers. Assuming that gastric and intestinal juices may contain some calcium chelating agents, the presence of phosphate was considered as a more representative system.

Figure 5 presents the swelling factors for the alginate/shellac (10/125 g/L) and alginate/eudragit (15/9 g/L) microcapsules versus the pH. Alginate/shellac capsules swell regularly from pH 2 to 8, up to a swelling factor 2,8. Alginate/eudragit capsules swell under pH 6 of a factor 3 then the swelling is intensified to reach up to 20 for pH 8. At pH 8, the structure of capsules is still visible but they are very soft. One would expect that intestine contraction would break the shell releasing the content.

Figure 6 shows that the swelling of the microcapsules are mainly linear with the time.

CONCLUSION

The production of oil core microcapsules with a shell composed of alginate and an enteric coating was demonstrated using the jet nozzle resonance method. In the formulation, alginate

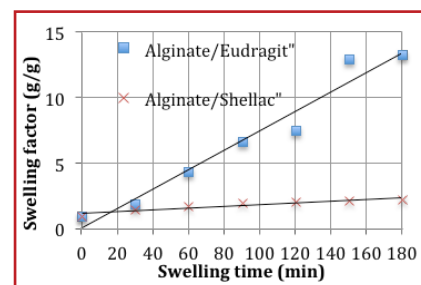


Figure 6 : Swelling of the microcapsules versus time

insures the gelation while shellac and eudragit provides enteric properties. Both alginate/shellac and alginate/eudragit FS30D formulation allow to get spherical and mono-core capsules by selecting carefully the operating conditions. In-vitro, the swelling behavior of alginate/eudragit capsules is more promising that alginate/shellac. However, these results have to be confirmed by in vivo test.



REFERENCES

- Whelehan, M.; Marison, I. Liquid-core microcapsules as a novel methodology for the extraction of pesticides and pharmaceutically active compounds from water. *New Biotechnology* 25, S264-S264 (2009)

Addresses

Authors thanks for their support the ITMOCancer/INSERM and REDES-CO-NICYT (project 130015).

¹ Oniris, 44322 Nantes, France

² Universidad de la Frontera, Temuco, Chile

³ INRA Toxalim, Toulouse, France

⁴ Norevo, Hamburg, Germany



Aurélie Bidoret

Oniris, 44322 Nantes, France

aurelie.bidoret@oniris-nantes.fr

FABRICATION OF METHACRYLATE ALGINATE BEADS FOR BIOENCAPSULATION OF CELLS

Li, P.¹, Müller, M.¹, Frettlöh, M.² and Schönherr, H.¹

INTRODUCTION & OBJECTIVES

Biosensors, which combine biological components with physicochemical detectors, are widely used for monitoring bioavailable analyte concentrations in environmental, medical, and toxicological applications. Apart from enzyme-responsive systems (Haas, 2015; Sadat Ebrahimi, 2014), whole cell biosensors show high specificity, sensitivity and portability (Gasparini, 2014). A common procedure for producing immobilized whole cell biosensors is based on silica sol-gel chemistry and calcium cross-linked alginate beads. However, encapsulation in silica is limited by detrimental effects on cell viability. The natural biopolymer alginate is biocompatible, but these matrices suffer from disruption in water as well as from inherent biodegradation, which cause the leakage of cells inside of the beads. In order to keep control on microbeads swelling and cell leakage, here we used glycidyl methacrylate-functionalized alginate (GMSA), which can be cross-linked by UV-irradiation to form microbeads.

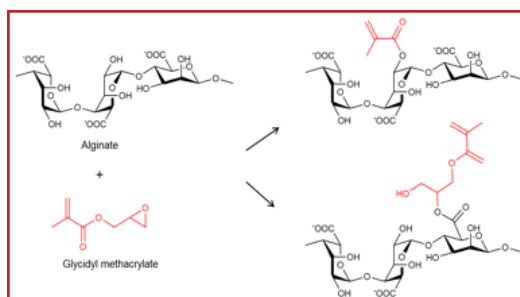


Fig.1. Methacrylation of SA to yield macromer GMSA by a competition reaction between ring opening and transesterification.

Preparation of GMSA microbeads

Electro jetting was used to fabricate microbeads. After dissolving 2 wt% GMSA and 0.1 wt% Irgacure 2959 (2-hydroxy-4'-(2-hydroxyethoxy)-2-methylpropiophenone, Sigma) in 10 mM Tris buffer (pH=8.5), the solution was transferred into syringe carefully to avoid air bubble. Then the solution in the syringe was extruded through the needle by the force of electric field and dropped into 100 mM CaCl₂ in Tris buffer (10 mM, pH 8.5), which also contains 0.1 wt% Irgacure 2959.

Fluorescence labeling of GMSA

GMSA was fluorescently labelled with fluoresceinamine (isomer I, Sigma) using EDC (N-[3-Dimethylaminopropyl]-N'-ethylcarbodiimide hydrochloride, Sigma) and Sulfo-NHS (N-hydroxysulfosuccinimide sodium salt, Sigma).

Characterization of GMSA microbeads

The optical images of the beads were taken with a Primo Vert light microscope (Zeiss). The fluorescence microscopy images of the beads were taken with an Axio-

vert 135 fluorescence microscope (Zeiss). Scanning electron microscope (SEM) imaging was performed with a CamScan 24 with an accelerating voltage of 10 kV, after sputter-coating the samples with gold. The SEM samples were prepared using the critical point drying method.

Stability test of GMSA and SA beads

After hardening in CaCl₂ solution for 1 hour, 4 wt% GMSA beads were firstly irradiated under UV for 5 min (CL-1000 series UV crosslinker, with CL-1000L Model 365 nm UV tubes, 5 × 8 w), then filtered by a filter with mesh size of 30 μm, washed with Tris buffer for 3 times, immersed into 10 mM or 100 mM CaCl₂ in Tris buffer solution (10 mM, pH 8.5), respectively, for 7 days. Light microscopy images of microbeads before and after immersing in solutions of different concentration of CaCl₂ were taken to measure and compare the diameters of the beads.

RESULTS & DISCUSSION

While the exact mechanism could not be well confirmed in this study yet, it is likely that glycidyl methacrylate reacts with sodium alginate (SA) by a competition reaction of ring opening and



MATERIAL & METHODS

Synthesis of GMSA macromer

Methacrylate-functionalized alginate was synthesized by the addition of glycidyl methacrylate (Sigma, ~12-fold excess) to a solution of 1 wt% alginic acid sodium salt (Sigma, MW = 120 - 190 kDa) in deionized water and reacted at room temperature for 24 hours. The macromer solution was precipitated twice in a large excess of acetone (20 times the volume of the reaction solution), filtered and dried under vacuum.

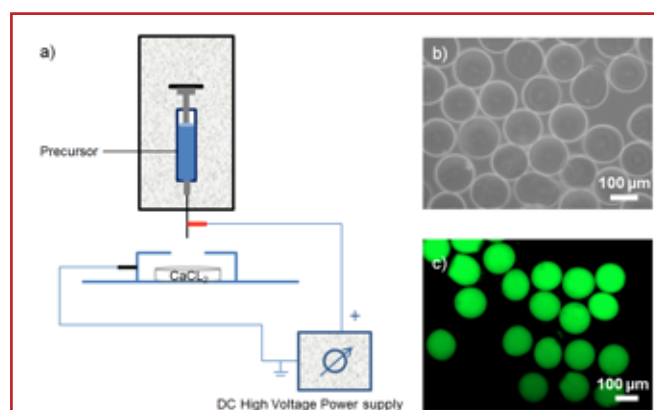


Fig.2. a) Scheme of electro jetting set up used for fabricating beads; b) light microscope image of 2 wt%GMSA beads; c) fluoresceinamine labelled 2 wt%GMSA beads.

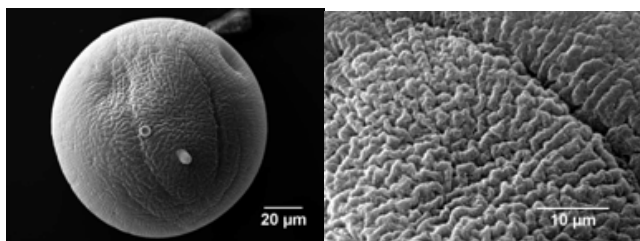


Fig.3. SEM images of GMSA beads.

transesterification [Bencherif, 2008], as shown in Fig. 1. ¹H-NMR spectroscopy confirmed the methacrylate functionalization of SA, showing signals at ~ 5.6 and ~6.1 ppm (acrylate) and signals at ~1.9 ppm (methyl group). In the presence of the photoinitiator Irgacure 2959, GMSA macromer solutions formed bulk hydrogels after exposure to UV-light. After methacrylate functionalization, the polymer is known to be biocompatible, non-toxic and cell friendly [Baier, 2003].



The sizes and shapes of GMSA microbeads produced by electro jetting (Fig.2a) were related to the voltage adapted, the polymer concentration, electricity, viscosity and surface tension of solution. For 2 wt% GMSA, when an electrical potential of 6.0 kV was applied, regular spherical microbeads with a narrow size distribution of less than 200 μm were produced (Fig.2b). To future study the polymer distribution in the beads, GMSA was fluorescently labelled by covalent binding of the amino group of fluoresceinamine to the carboxylic groups of GMSA using carbodiimides (Fig. 2c). The polymer gradient in GMSA beads can be evaluated by confocal laser scanning microscopy, and the bead diameters can be quantified by fluorescence spectroscopy.

Scanning electron microscopy was used to study the surface morphology of GMSA microbeads, as demonstrated in Fig. 3. Due to the dehydration during the sample preparation process, the diameters of beads were reduced to 110 ± 10 μm, while the spheres retained their overall

shape.

The investigation of the stability of the beads includes test of the swelling properties of beads and molecule permeability. Here the first test of swelling properties of beads were done by immersing beads into

solutions of different concentration of CaCl₂, and by comparing the changes in bead diameter. After 7 days, the mean value of bead diameter in 10 mM CaCl₂ solution was 203 μm, in 100 mM CaCl₂ solution it was 203 μm, while the mean diameter after hardening was 200 μm.

CONCLUSIONS & PERSPECTIVES

The diameter distribution of beads from methacrylate functionalized alginate formed via electro jetting method was less than 200 μm. After hardening in CaCl₂ solution, beads were further chemically cross-linked under UV irradiation to optimise the swelling properties of beads. GMSA was labelled with fluoresceinamine to investigate the polymer gradient by confocal laser scanning microscopy. The first swelling test of GMSA beads was done by immersing beads into different concentration of CaCl₂ solution. After 7 days, the diameter of the beads kept nearly constant. In the future, bacteria will be encapsulated into the beads to test the cytotoxicity of GMSA beads. Hence for the first time a protocol for the fabrication of methacrylate-alginate beads has been established, which possesses considerable potential to provide stable, reproducible

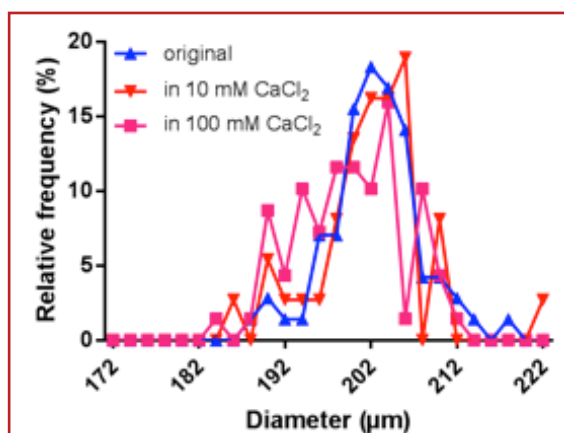


Figure 4: Fluorescence distribution of cells exposed to PMMA- and PCL-based NPs with siRNA.

bioencapsulation of cells.

REFERENCES

- Haas, S. et al. Enzyme degradable polymersomes from hyaluronic acid-block-poly (ε-caprolactone) copolymers for the detection of enzymes of pathogenic bacteria, *Biomacromolecules* 16, 832–841 (2015).
- Sadat Ebrahimi, Mir Morteza & Schönherr, H. Enzyme-sensing chitosan hydrogels, *Langmuir: the ACS journal of surfaces and colloids* 30, 7842–7850 (2014).
- Gasperini, L., Mano, J.F., and Reis, R.L. Natural polymers for the microencapsulation of cells. *J. R. Soc. Interface* 11, 20140817 (2014).
- Bencherif, S. A. et al. Influence of the degree of methacrylation on hyaluronic acid hydrogels properties, *Biomaterials* 29, 1739–1749 (2008).
- Baier Leach, J. Bivens, K. A. Patrick Jr. C. W. & Schmidt, C. E. Photocrosslinked hyaluronic acid hydrogels: Natural, biodegradable tissue engineering scaffolds, *Biotechnol. Bioeng.* 82, 578–589 (2003).

Acknowledgement

The authors thank Dipl.-Ing. Gregor Schulte for technical supports concerning electro jetting setup. The authors would like to acknowledge financial support from the EU (ERC project ASMIDIAS, Grant no. 279202) and in particular funding received for the project from the funding program of the Federal Ministry of Economics and Technology in Germany, "Central Innovation Programme SME" (ZIM, KF2589507SK4), that is carried out together with our cooperation partner Quh-Lab (Siegen).

¹ Physical Chemistry I, University of Siegen, Adolf-Reichwein-Str. 2, 57076, Siegen.

² Quh-Lab Lebensmittelsicherheit, Siegener Str.29, 57080, Siegen.



Ping Li

Physical Chemistry I, Univ. of Siegen, Adolf-Reichwein-Str. 2, 57076, Siegen, Germany
ping.li@chemie.uni-siegen.de

CHITOSAN COATING AS AN OPSONIZATION CIRCUMVENT STRATEGY FOR PLGA NANOPARTICLES

Oliveira C.¹, Veiga F.², Ribeiro A. J.¹ - ¹IS & BMC, Porto, Portugal; ²CNC, Coimbra, Portugal.

INTRODUCTION & OBJECTIVE

Nanoparticles composed of biodegradable and biocompatible materials, such as poly(lactic-co-glycolic acid) (PLGA) are highly attractive in nanomedicine and are considered an auspicious field of research with regard to their translational potential. However, systemic delivery has been a significant bottleneck to the development of nanoparticle-based formulations due to the interactions established between nanomaterials and the biological environment. These are governed by the physicochemical and morphological properties of the delivery system that impact on the dynamics of differential protein adsorption that modulate the clearance rate from the systemic circulation and impact on biocompatibility. Several strategies have been adopted to confer stealth properties to delivery systems by circumventing uptake by the reticuloendothelial system. Among the latter, chitosan coating [Amoozgar, 2012] and the use of the surfactant poloxamer 188 [Jain, 2013] have been proposed for PLGA nanoparticles as alternatives to PEGylation. As polymer characterization has been previously set forth to improve the reproducibility and standardization of the bioencapsulation process [de Vos, P., 2009], we focus on the interactions of polymers within a biological environment which modulate their *in vivo* behavior. Even though *in vitro* characterization

has been improved to anticipate the biokinetics of delivery systems upon intravenous injection, lack of standardized assays compromises the comparability of different strategies and *in vitro-in vivo* correlation, enhancing the need for improved assessment under representative conditions. Therefore, we report the *in vitro* characterization of chitosan-coated and uncoated PLGA nanoparticles with the aim of contributing to the establishment of standardized *in vitro* settings that allow time and resource-efficient optimization.



MATERIALS & METHODS

PLGA (Resomer® RG 502 H, Evonik Industries, Germany) nanoparticles were prepared through a nanoprecipitation method. Briefly, an extra-pure acetone [Scharlau, Spain] solution of PLGA (15 mg/mL) was added dropwise into a 0,5% (w/v) aqueous solution of poloxamer 188 (Kolliphor P188, Basf SE, Germany), under magnetic stirring. Acetone was removed by rotoevaporation. Particles were centrifuged and the pellet washed twice with MilliQ water and resuspended in an aqueous solution of poloxamer 188.

Chitosan coating was achieved by addition of a 0,025% (w/v) chitosan (Low molecular weight chitosan, Sigma-Aldrich, USA) in 0,5% (v/v) lactic acid (VWR, USA) solution (pH 4,6) to PLGA nanoparticles, under sonication. The resulting particles were centrifuged and washed twice using centrifugal filters with 100 kDa MWCO (Ultracell-15, Millipore, Germa-

ny) and resuspended in MilliQ water. The amount of chitosan adsorbed to PLGA nanoparticles was quantified using the ninhydrin reagent (Sigma-Aldrich, Germany), according to a method previously described [Leane et al, 2004].

Particles were characterized according to size and zeta potential using a Zetasizer Nano ZS (Malvern Instruments, UK). Bovine serum albumin (BSA) (Sigma-Aldrich, Germany) in phosphate buffer saline (PBS) pH=7,4 (0,4 mg/mL) was used to assess opsonization, by incubation of nanoparticles with the previous solution at a ratio of 9:1 at 37°C using a water bath under agitation of 150 strokes/min. The extent of protein adsorption to nanoparticles was quantified using the Coomassie Plus assay (Thermo Fisher Scientific, USA).

RESULTS & DISCUSSION

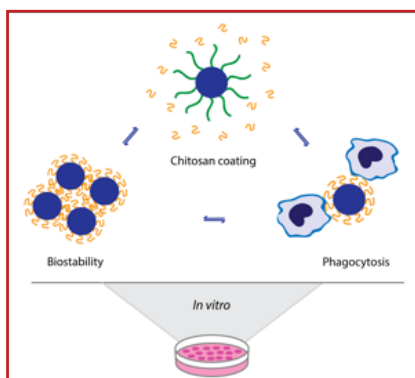
1. Nanoparticle preparation and chitosan-coating

A. Characterization of nanoparticles

Table 1 presents mean values and standard deviation of three consecutive runs. Chitosan-coated PLGA nanoparticles were prepared in triplicate and PLGA nanoparticles are the combination of seven batches

B. Quantification of chitosan adsorbed to PLGA nanoparticles

The quantification of the amount of polymer at the surface of nanoparticles improves the comparability of results but is often lacking in characterization studies. Herein, chitosan was added to PLGA nanoparticles to a final concentration of 0,3 mg/mL. The efficiency



Graphical abstract. *In vitro* predictability of the biostability and accelerated clearance of PLGA nanoparticles modulated by chitosan-coating.

Table 1. Characterization of the size and surface charge of PLGA nanoparticles and chitosan-coated PLGA nanoparticles.

Formulation	Mean diameter (nm)	Polydispersity index	Zeta potential (mV)
PLGA NP	225,33 ± 1,01	0,216 ± 0,009	-31,9 ± 0,818
Chitosan-coated PLGA NP	358,35 ± 37,14	0,192 ± 0,007	+58,8 ± 3,944

ARTICLE



Figure 1. Ninhydrin assay for the quantification of chitosan. The determination of coating efficiency was performed in triplicate (last 3 samples from the right)

of the coating process was assessed through quantification of the amount of chitosan adsorbed to PLGA nanoparticles through the ninhydrin assay (Figure 1). Chitosan was determined to be at a concentration of $0,202 \pm 0,01$ mg/mL, indicating that the coating process was efficient with approximately 67,3% of chitosan adsorbed to the surface of PLGA nanoparticles. These results are corroborated by the increase in size and inversion of zeta potential, evidenced in Table 1.

2. In vitro characterization of the stability of nanoparticles and opsonization

A. Stability in a biological environment

The stability of PLGA and chitosan-coated PLGA nanoparticles was evaluated by means of size evolution upon incubation in a BSA solution, one of the most abundant proteins in plasma, mimicking the opsonization process. As represented in Figure 2, PLGA nanoparticles were stable maintaining a similar size distribution profile as before the assay, whereas chitosan-coated PLGA nanoparticles evidenced a significant increase in particle size, with mean diameter values shifting to above 1 μm .

B. Evaluation of the extent of opsonization of PLGA and chitosan-coated PLGA nanoparticles

Opsonization was assessed by means of adsorption of BSA to the surface of nanoparticles after incubation in the same conditions used for stability studies, at a final protein concentration of 40

$\mu\text{g/mL}$. The adsorption of BSA onto the surface of nanoparticles was quantified by the Bradford assay which evidenced negligible ($<1 \mu\text{g/mL}$) adsorption of BSA to PLGA nanoparticles. In contrast, chitosan-coated PLGA nanoparticles were subject to significant opsonization demonstrated by a BSA concentration of $6,87 \pm 2,28 \mu\text{g/mL}$, approximately 17,2% of total protein. Measurements were performed in triplicate and are represented as mean values and standard deviation. Incubation of samples in PBS was used as control.



CONCLUSIONS

PLGA nanoparticles demonstrated higher stability and ability to circumvent BSA adsorption in comparison to chitosan-coated PLGA nanoparticles. The improved behavior of PLGA nanoparticles might be attributed to the effect of poloxamer 188 in the formulation, which has been previously shown to be efficient in evading phagocytosis by macrophages in vitro (Jain, 2013).

The decreased ability of chitosan to circumvent opsonization, in contrast to previous studies (Amoozgar, 2012) may be related to the use of a polymer with higher molecular weight in this study. Indeed, the hydrophobicity of chitosan has been correlated to its molecular weight, evidencing an important parameter that influences opsonization, as the forces that govern the interaction between chitosan and BSA are predominantly hydrophobic (Bekale, 2015).

The assays here presented have been

previously described to the characterization of nanoparticles in different contexts, evidencing the lack of standardization that contributes to lab to lab variation. We have applied these methodologies for the study of an important subject in the field of nanobio interactions strengthening their potential as relevant tools for a first screening approach to the behavior of nanoparticles in a biological environment. As a future step, we expect to evidence other parameters that influence the in vitro study of opsonization as well as to evaluate this phenomenon using higher complexity in vitro models, namely macrophage cell lines, in order to correlate both stages of in vitro studies which may contribute to the improvement of efficiency and biocompatibility assays.

REFERENCES

- Amoozgar, Z., Park, J., Lin, Q. & Yeo, Y., Low molecular-weight chitosan as a pH-sensitive stealth coating for tumor-specific drug delivery, *Mol. Pharm.*, 9, 1262-1270 (2012)
- Bekale, L., Agudelo, D. & Tajmir-Riahi, H.A. Effect of polymer molecular weight on chitosan-protein interaction. *Colloids Surf. B Biointerfaces* 125, 309-317 (2015).
- de Vos, P., Bucko, M., Gemeiner, P., et al. Multiscale requirements for bioencapsulation in medicine and biotechnology. *Biomaterials* 30, 2559-2570 (2009).
- Jain, D., Athawale, R., Bajaj, A., et al., Studies on stabilization mechanism and stealth effect of poloxamer 188 onto PLGA nanoparticles, *Colloids Surf. B Biointerfaces*, 109, 59-67. (2013),
- Leane, M. M., Nankervis, R., Smith, A. & Illum, L. Use of the ninhydrin assay to measure the release of chitosan from oral solid dosage forms. *Int. J. Pharm.* 271, 241-249 (2004).

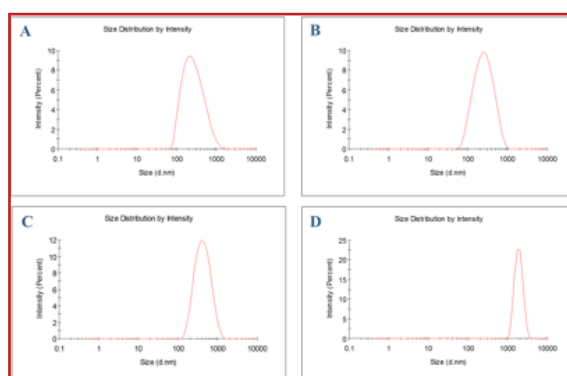


Figure 2. Size evolution of PLGA and chitosan-coated PLGA nanoparticles after incubation at 37°C for 1 hour in a BSA solution in PBS pH=7,4 at a ratio of nanoparticles to BSA solution of 9:1. Size distributions of PLGA nanoparticles before (A) and after (B) incubation as well as chitosan-coated PLGA nanoparticles before (C) and after (D) incubation are represented.



Claudia Oliveira
IBMC, University of Porto, Portugal
claudia.oliveira@ibmc.up.pt

FROM CO-APPLICATION TO CO-FORMULATION OF ENTOMOPATHOGENIC FUNGI

Przyklenk M., Hanitzsch M., Patel A., Univ Applied Sc. Bielefeld, Germany

Brandl M., Schumann M., Vidal S., Georg-August-University Goettingen, Germany

INTRODUCTION & OBJECTIVES

Soil-borne herbivorous insect pests like wireworms cause tremendous losses in potato fields. Entomopathogenic fungi (EPF) are considered as promising biocontrol agents in augmentative biocontrol strategies to control several soil born insects (Eckard et al. 2014). Furthermore, it is well known that larvae of many herbivorous insects, use CO₂ for host location (Bernklau and Bjostad, 1998), thus making CO₂ a promising attractant in combination with EPF.



Encapsulation offers a solution to many of the classical drawbacks in the application of EPFs, e.g. handling problems, low shelf life, poor establishment in soil and high costs due to high dosage per/ha.

Field trials in the past two years showed decreased damage to potato tubers due to wireworms, where the highest damage reduction was achieved by co-application of encapsulated fungus with CO₂ producing beads that acted as attract component in an "attract-and-kill" approach (Patel et al 2014). To enhance the application we are developing a co-formulation that includes *M. brunneum* spores and baker's yeast co-encapsulated in one bead within the project INBIOSOIL.

Here we report on the encapsulation and drying of novel EPF formulations as well as synergistic co-formulation of EPF with baker's yeast on lab and technical scale. Data will be presented on reduced biomass content, sporulation, CO₂ production, survival of dried encapsulated cells cross-linked with CaCl₂ or Ca-gluconate and shelf life.

MATERIAL & METHODS

Bead formation

Ca-alginate beads were prepared as described previously (Patel et al., 2014).

Sporulation of fungi

Sporulation of co-formulated *M. brunneum* was investigated by placing beads with different bead diameter on water agar (20 g agar with 1 L H₂O). The radial mycelium growth out of the beads was measured every three days and spores were scratched from the plate after 33 days with sterile dH₂O/Tween to determine CFU.

Measurement of CO₂

For the determination of CO₂ formation rates the amount of CO₂ produced by 1 g moist co-formulation beads was measured at 12°C, 20-22°C and 25 °C over 1 h in a 50 mL Tube. For the measurement of CO₂ in soil, boxes were filled up with peat soil (Fruhsdorfer Typ P) and 10 g of co-formulation were placed in 8 cm depth in the middle of each box. The soil humidity was periodically adjusted to 50 % (w/w) and the boxes were kept at room temperature at 20-22°C. CO₂ concentrations were measured using a portable pump-aspirated CO₂ measuring device (Vaisala, Finland).

Drying of formulations on lab and technical scale

The formulations were dried with a two-step drying method. In a first step 1 g moist beads were weighed on a piece of aluminum foil. The moist beads were dried overnight under the laminar air flow from a clean bench. In a second step the beads were dried in a desiccator for two more days. After drying, the a_w value of the beads was measured.

Survival of encapsulated cells (*M. brunneum* and baker's yeast) was determined by dissolving the beads as described previously (Patel et al., 2014) and counting CFU. Besides, a technical one-step drying process for different formulations with 30°C, 40°C and 50°C inlet temperature as well as a two-step process with a temperature profile were developed.



Statistical analysis

Statistical analyses were carried out with the software R version 3.1.1. All values are given as means ± standard deviations (SD). The influence of time on spore germination was tested for significance using Kruskal-Wallis test with the treatment as the independent variable. Averages of spore germination data were compared between treatments using the Mann-Whitney U post hoc range test.

RESULTS & DISCUSSION

Dry beads including co-encapsulated nutrients significantly increased the mean germination of spores out of the beads (Figure 1). Furthermore,

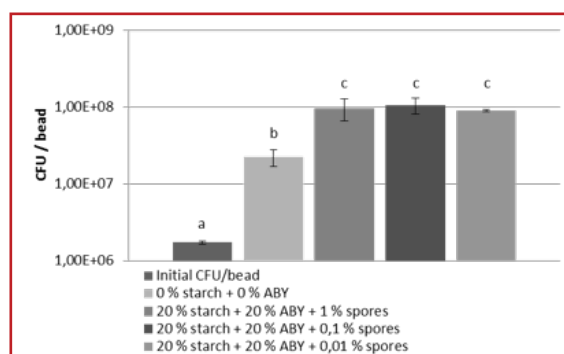


Figure 1: Sporulation of *M. brunneum* on water agar out of beads with different amounts of initial biomass loading, containing: Ca-alginate, *M. brunneum*, and corn starch. [Chi²=14.9, df=4, p<0.01]

ARTICLE

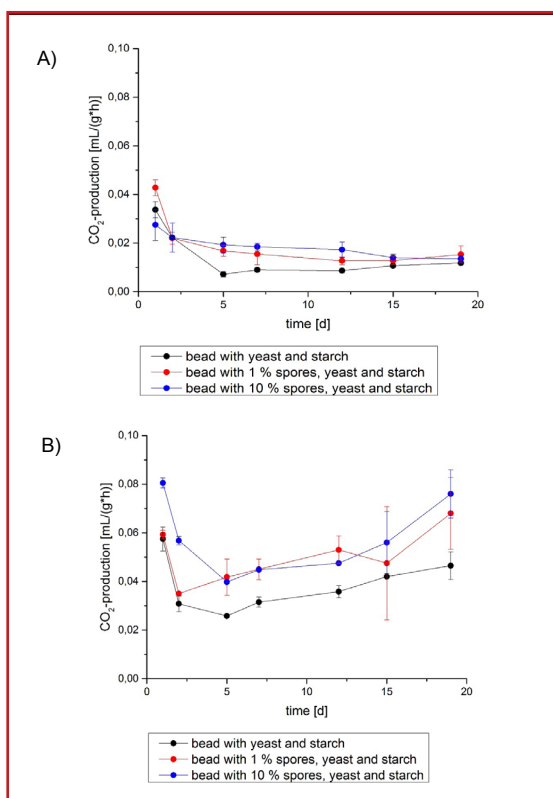


Figure 2: CO₂ formation rates over time. CO₂ formation rate in 50 ml tubes for co-encapsulated *M. brunneum* (1 % and 10 %) with baker's yeast at A) 12°C and B) 25°C. n = 3, S.D.

dry beads containing 1 % *M. brunneum* spores and dry beads with reduced biomass content showed no differences in mycelium growth (data not shown) and sporulation compared to the control.

This indicates that not all spores were able to germinate and to grow out of the bead, maybe due to diffusional limitations. However, the reduced biomass content enhances the cost-effectiveness of the formulation, e.g. if co-applied with CO₂ emitting beads containing baker's yeast.

In a next step we are developing a co-formulation realizing the "attract and kill" strategy using EPF and CO₂ within one bead.

The CO₂ production rates increases with higher temperatures in 50 ml tubes (Figure 2 A and B) as well as in soil. Beads containing spores produce about 1.5 more CO₂ at 25°C than beads without spores. Baker's yeast is not able to metabolize the starch included e.g. as a drying additive in the

bead. However, the encapsulated yeast benefits from the co-encapsulated fungi, which use amylases to break down the starch into monosaccharides. Furthermore, the CO₂ emission from the beads remained unchanged after a tenfold decrease of the spore amount.

A technical one-step drying process for 1 kg beads and ~50°C inlet temperature resulted in dried beads with 3.8% residual moisture, aw 0.2 and 13 % survival of *M. brunneum* and 26 % survival of baker's yeast (Figure 3).

Shelf life at two different temperatures 5 ± 2 °C and 25 ± 2 °C were carried out using non-water permeable Alu/PE bags filled with defined amounts of dried beads. Encapsulated spores were compared with free spores. Real time storage was performed for 6 months with regular sampling for CFU determination (data not shown).

First results of beads cross-linked with different concentrations of Ca-gluconate and dried in lab-scale process, showed increased cell survival up to 80%, two times more than beads which were cross-linked with CaCl₂, indicating that Ca-gluconate can act as osmoprotectant (data not shown.)

CONCLUSIONS & PERSPECTIVES

To conclude, we developed formula-

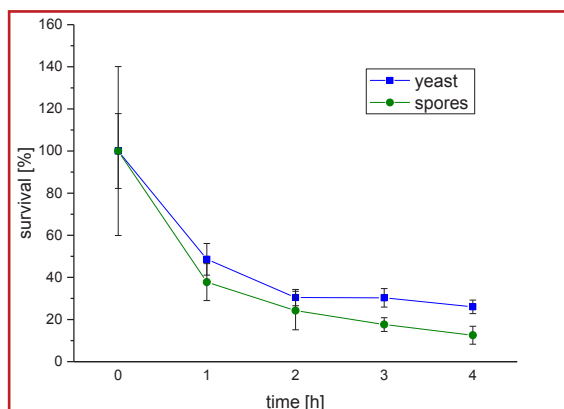


Figure 3: Survival of *M. brunneum* and baker's yeast, dried in a fluidized bed dryer.

tions and co-formulations with high survival, sporulation, shelf life and CO₂ formation. Firstly the EPF bead with *M. brunneum* spores as co-application with CO₂ producing beads containing baker's yeast and secondly, we co-encapsulated EPF with baker's yeast and starch in one bead. EPF beads with a reduced biomass content to increase cost effectiveness were developed. In an on-going experiment the co-encapsulated beads with *M. brunneum* and baker's yeast (2 % Ca-alginate, aerospores from *M. brunneum*, 16.7 % baker's yeast and 20 % starch) with CO₂ releasing properties are tested against the larvae of wireworms in potato field trials at seven locations. Furthermore we are investigating Ca-gluconate as crosslinker and its potential to act as osmoprotectant during the drying process.

REFERENCES

- Bernklau E.J., and Bjostad L.B. 1998: Behavioral Responses of First-Instar Western Corn Rootworm (Coleoptera: Chrysomelidae) to Carbon Dioxide in a Glass Bead Bioassay. *Entomological Society of America*, Vol. 91, no. 2, pp: 444-456
- Eckard S., Ansari M.A., Bacher S., Butt T.M., Enkerli J., Grabenweger G., Virulence of in vivo and in vitro produced conidia of *Metarhizium brunneum* strains for control of wireworms. *Crop Protection* 64 (2014) 137-142
- Patel A., Przyklenk M., Humbert P., Brandl M., Vemmer M., Hanitzsch M., Schumann M., and Vidal S., 2014. Encapsulation and drying of *Metarhizium brunneum* as basis for an attract and kill strategy. XXII International Conference on Bioencapsulation (Bioencapsulation Research Group – 17-19.09.2014 – Bratislava)



Michael Przyklenk

University of Applied Science Bielefeld, Engineering and Mathematics, Wilhelm-Bertelsmann-Straße 10 Germany
michael.przyklenk@fh-bielefeld.de

SPONTANEOUS CO-ASSEMBLY OF PROTEINS FOR ENCAPSULATION OF A HYDROPHILIC VITAMIN

Chapeau A.L.¹, Tavares M.G.^{1,2}, Hamon P.¹, Croguennec T.¹, Poncelet D.³, Bouhallab S.*¹

INTRODUCTION

Encapsulation of bioactive compounds such as vitamins and micronutrients is a great challenge to develop new functional foods. There is a growing demand from consumers for food products offering health benefits such as products enriched with vitamins. At the same time, consumers tend to favor natural food or products with minimal amount of additives. The encapsulation of bioactives usually resorts to extraneous components that are not natural constituents of the targeted food product. It could therefore be relevant to seek to encapsulate bioactive molecules by means of intraneous components that are natural constituents of the targeted food product.



Among food constituents, food proteins are biopolymers that appear suitable for the transport and protection of several bioactives. Recent studies have reported the ability of two oppo-

sitely charged milk proteins, beta-lactoglobulin (BLG) and lactoferrin (LF), to spontaneously co-assemble to form heteroprotein complexes called "coacervates" (Anema et al., 2014; Tavares et al., 2015). Complex coacervation is a well-known phase separation between two oppositely charged macromolecules, into a concentrated phase of coacervates and dilute phase. It can be used as an encapsulation technique. In the literature, two general procedures can be found to encapsulate a compound by the complex coacervation of two biopolymers.

The objective of this work is to investigate the potentialities of coacervates entirely made from food proteins to encapsulate a bioactive compound according to these procedures. We investigated the potentiality of BLG-LF coacervates to encapsulate the hydrophilic vitamin B9 (B9).

MATERIALS & METHODS

Encapsulation of B9 by BLG-LF co-assembly.

LF and BLG were mixed with B9 following the encapsulation procedure by coacervation (Fig. 1). B9 was mixed either with BLG or LF at a certain ratio and controlled pH. After ten minutes, the other protein was added to the system either at the same initial pH or after a drop of pH. All systems were mixed at room temperature. A range of mixing ratios, and pH conditions were tested according to a screening experimental plan in order to determine the ratios and pH conditions that lead to B9-BLG-LF co-

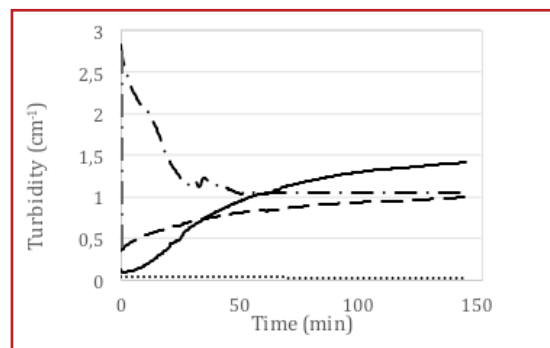


Figure 2: Time turbidity of B9-BLG-LF co-assembly.

Characterization of the B9-BLG-LF co-assembly.

Co-assembly of B9-BLG-LF was assessed by turbidity measurements. Co-assembly formation and final shapes of the encapsulated systems were followed by phase contrast microscopy (micrographs) and live phase contrast microscopy (films).

B9 loading capacity of B9-BLG-LF co-assembly.

Mixed systems of B9-BLG-LF were centrifuged at 28 000g for 30 min. Concentrations of B9, BLG and LF in the supernatants were determined by RP-HPLC and used to determine the remaining concentrations into the pellet by subtraction. These fractions were used to calculate two key parameters of the co-assembly, the co-assembly formation and its loading capacity for B9, according to the following equations:

$$\text{Co-assembly formation} = \frac{M_{\text{co-assembly}}}{M_{\text{initial}}} = \frac{M_{\text{B9}} + M_{\text{MLF}} + M_{\text{MBLG}}}{M_{\text{B9}} + M_{\text{MLF}} + M_{\text{MBLG}}}$$

$$\text{B9 Loading capacity} = \frac{M_{\text{B9}}}{M_{\text{co-assembly}}} = \frac{M_{\text{B9}}}{M_{\text{B9}} + M_{\text{MLF}} + M_{\text{MBLG}}}$$

RESULTS & DISCUSSION

Effect of initial pH and mixing ratio on B9-BLG-LF co-assembly

Turbidity measurements presented three different kinetics profiles according to pH conditions and mixing ratio

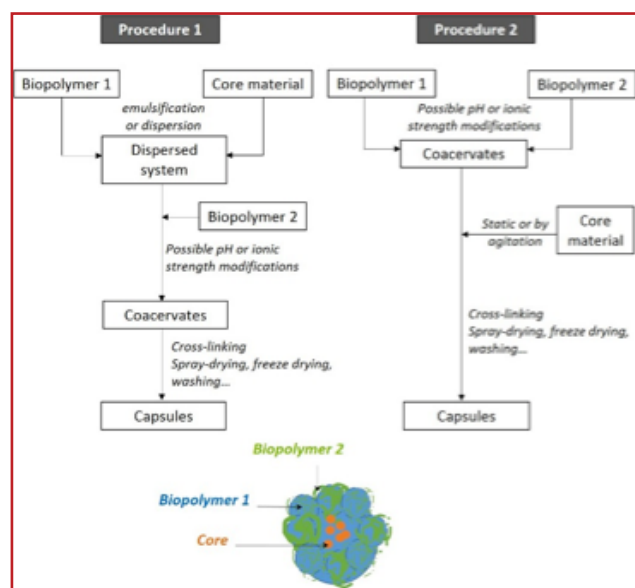


Figure 1: General procedures used to encapsulate a core molecule by the complex coacervation of two biopolymers.

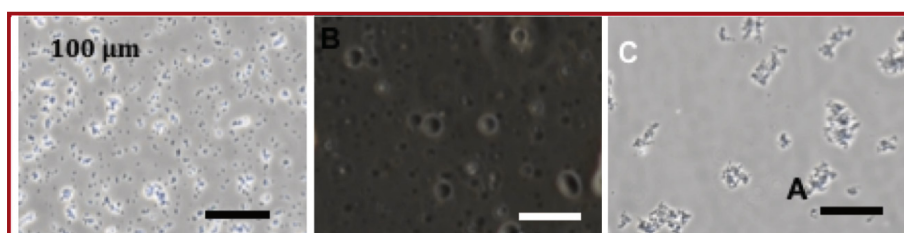


Figure 3: Phase contrast microscopy micrographs of B9-BLG-LF co-assembly, 1cm = 100μm.

(Fig. 2): two profiles where turbidity increased over time up to a maximum and one profile where turbidity is maximum with BLG introduction and then decreased. In addition, the control series show no turbidity. This suggests that, the increase of turbidity may be associated with BLG and LF spontaneous co-assembly in presence of B9.

According to the micrographs of the three turbid systems (Fig. 3), we identified three different types of B9-BLG-LF co-assembly: small aggregates (A), large aggregates (B) and microspherical coacervates (C). Linking micrographs with turbidity profiles, it can be deduced that B9-BLG-LF self-aggregation has a rather low kinetics compared to B9-BLG-LF complex coacervation which happened spontaneously with BLG introduction and lead to the formation of microsphere coacervates. As the turbidity decreased, the coacervate phase is probably unstable.



Co-assembly by complex coacervation is a spontaneous phenomenon which occurs through electrostatic interactions between two oppositely charged biopolymers and can lead, depending on the system, to microspheres formation (Yan et al., 2013). Micrographs in Fig. 4 showed the microspheres formation by complex coacervation resulting from adding BLG to a mixed system of LF and B9. We evidenced the growth of

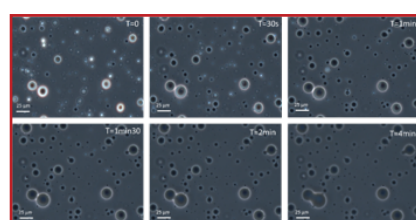


Figure 4: B9-BLG-LF microspheres formation by live phase contrast microscopy, 1cm=25μm.

microspheres over time, until 5 μm diameter for the smallest and 25 μm diameter for the biggest within 5min.

B9-BLG-LF microspheres formation by complex coacervation

Co-assembly by complex coacervation is a spontaneous phenomenon which occurs through electrostatic interactions between two oppositely charged biopolymers and can lead, depending on the system, to microspheres formation (Yan et al., 2013). Micrographs in Fig. 4 showed the microspheres formation by complex coacervation resulting from adding BLG to a mixed system of LF and B9. We evidenced the growth of microspheres over time, until 5 μm diameter for the smallest and 25 μm diameter for the biggest within 5min.

Table 1: Co-assembly formation and B9 loading capacity of B9-BLG-LF co-assembly in situation of microspheres formation

B9/Total protein	Co-assembly formation	B9 Loading capacity
4/3	0.87	0.64
6/3	0.89	0.73
10/3	0.92	0.81
4/11	0.93	0.60
6/11	0.94	0.70
10/11	0.95	0.91

Loading capacity of B9-BLG-LF microspheres.

Table 1 evidenced that for a fixed total protein content, microspheres formation by co-assembly [1] was promoted by an increase of B9. Loading capacity of microspheres [2] ranged from 0.60 to 0.91 depending on the B9/total protein ratios. The higher loading capacity is obtained for the higher microspheres formation. This indicates that, B9-BLG-LF microspheres co-assembly may be viewed as a viable loading system to encapsulate B9.

CONCLUSION & PERSPECTIVES

BLG and LF are able to spontaneously co-assemble with B9 into aggregates or coacervates depending on the mixing ratio and pH. Coacervates are obtained by the complex coacervation process and lead to the formation of microspheres. B9-BLG-LF microspheres present a high loading capacity for B9. These results demonstrate that BLG-LF microspheres can be used to encapsulate a hydrophilic bioactive compound by complex coacervation. Now, the stability of these structures has to be investigated. These co-assembly has potential to improve the nutritional characteristics of a food product while ensuring its naturality as whey proteins are used as encapsulating agents.

REFERENCES

- Anema S.G. and de Kruif C.G., 2014. Complex coacervates of lactotransferrin and β -lactoglobulin. *J. Colloid Interface Sci.* 430, 214–220.
- Tavares G.M., Croguennec T., Hamon, P., Carvalho A.F., Bouhallab S., 2015. Selective coacervation between lactoferrin and the two isoforms of beta-lactoglobulin. *Food Hydrocoll.* 48, 238–247.
- Yan Y., Kizilay E., Seeman D., Flanagan S., Dubin P.L., Bovetto L., Donato L., Schmitt C., 2013. Heteroprotein Complex Coacervation: Bovine β -Lactoglobulin and Lactoferrin. *Langmuir* 29, 15614–15623.

ACKNOWLEDGEMENT

We thank BBA association, UMR STLO, Regional councils of Brittany and Pays de la Loire, PROFIL project, carried out by « Pole Agronomique Ouest ».

¹Agrocampus Ouest, UMR1253, 35042 Rennes, France

²Laboratory Research in Milk Products, Vicoso, Brazil.

³ONIRIS, 44322 Nantes, France.



Anne-Laure Chapeau

Agrocampus Ouest, UMR1253, 35042 Rennes, France
annelaure.chapeau@rennes.inra.fr

CONTROL OF ULTRA-HIGH VISCOSITY AS A POWER-FUL PARAMETER FOR ALGINATE CAPSULES

Schulz, A., Gentile, L., Zimmermann H., Fraunhofer IBMT, Germany; Dobringer, J., Vásquez, J., UCN, Chile.

INTRODUCTION & OBJECTIVE

Among the numerous polymers with natural and synthetic origin, alginate is one of the most dominantly applied polymers in encapsulation (de Vos, 2009). Alginates are unbranched anionic polysaccharides extracted from cell walls of brown algae. Consisting of 1,4-glycosidically linked β -D-mannuronic acid (M) and α -L-guluronic acid (G) units, the alginate's structure is arranged in consecutive (MM, GG) and alternating (MGMG) blocks. The composition and sequential structure together with the molecular weight vary depending on the species of algae, the processed plant tissue, seasonal conditions as well as the algae's habitat and age. Since the alginate's chemical composition determines the capsule properties and functionality, reliable characterizations of growth areas require an accurate documentation of the existing conditions, in particular the geographical location, water analysis and weather data such as temperature and moisture. Commercial alginates are often extracted from algae washed ashore by the surf and the wind resulting in a blend with unspecified natural origin and growth conditions. This algal material is dried on the ground or blankets for several days exposed to UV radiation and contaminations of bacterial, fungal, animal and anthropogenic components which lead to cytotoxic, mitogenic and apoptosis-inducing impurities. Following antimicrobial procedures including UV irradiation and high temperatures generate low-molecular alginate. Since the viscosity and the biocompatibility both increase with molecular mass, common proceedings are limiting the success of the capsule. It is important to note that very often alginates of extremely low viscosity are studied. Ultra-high viscosity (UHV) alginates provide favorable characteristics in terms of chemical and mechanical stability required for successfully applied bioencapsulations. Here, a constant quality of the capsule material is crucial, gained by the standardization and validation

of the entire manufacturing process from the material production site to the final bioencapsulation.



MATERIALS & METHODS

Harvest, transport & preparation of algal material

UHV alginates are obtained from stipes of the brown algae *Lessonia nigrescens* (LN) and *Lessonia trabeculata* (LT) harvested freshly and directly from the sea. LN grows in the tidal zone at the Chilean coast exposed to high surf resulting in an assimilation of the plant to very elastic and flexible stipes consisting of high M alginate (~60%). In contrast, LT grows in subtidal habitats with very stiff stipes and high G alginate (~90%). Due to various conditions in different areas of harvest, the geographical origin of the natural sample as well as its tracking are enabled using the satellite-based global positioning system GPS. Collected algae are sealed in UV-protective bags and monitored in respect of the temperature and the humidity during the whole process. The harvested stipes are peeled to remove bacterial components with the peel, subjected to antimicrobial treatment, chopped and gently dried until a residual moisture of $rH \leq 0.5\%$. Prepared algal material is stored in a defined vacuum environment.

Alginate extraction

After improving the purity of the material using oxygen-plasma sterilization, high M alginate is extracted with iminodisuccinate, whereas high G alginate is best extracted with ethylene-diaminetetraacetic acid after a hydrochloric acid treatment. The extracted alginates are purified by the removal of

cell debris via several filtration steps. Furthermore, phenols, fucoidan, low molecular weight oligomers, proteins and endotoxins are removed by successive alginate precipitations in ethanol (Zimmermann, 2007). Beside the standardized process, LT alginate extractions avoiding the acidic treatment are carried out. Moreover, extractions of alginate out of fresh and dried algal material are compared.

Alginate characterization

To determine the chemical composition and sequential structure of alginates 1H-NMR spectroscopy is applied. Taking spectra of alginate in D2O at 70 °C and 500 MHz, the monomer composition as well as diad and triad frequencies are measured. The dynamic viscosity of 0.65% w/v (weight per volume) alginate solution is examined at 20 °C and a shear rate of 1 s^{-1} using Anton Paar Rheometer Physica MCR 301. The extracted alginate is characterized in terms of its sterility (CASO-Bouillon and Thioglycolat-Bouillon), bacterial endotoxins (limulus amoebocyte lysate test) and protein content (Warburg-Christian).

Ultraviolet treatment of algae

The impact of UV radiation on the characteristics of algal material is investigated by UV treatment (365 nm, 400-500 W) of LN (processed according to standardized operating procedure as described above) for 0, 1, 3, 6 and 10 h. Then, UV irradiated algae are extracted and dissolved to 0.7% w/v alginate solution followed by dynamic viscosity measurements at 20 °C and 1 s^{-1} .



Capsule formation

Microcapsules are made from 1:1 mixtures of UHV alginate extracted from LN and LT. The 0.65% w/v alginate solution is dispersed into small droplets using coaxial air stream tech-

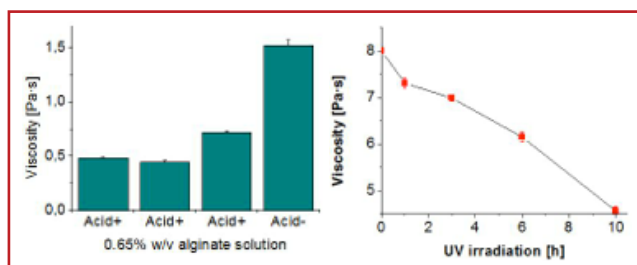


Figure 1: left: The avoidance of acids (Acid-) results in increased alginate viscosity compared to acidic treated samples (Acid+). right: Alginate's viscosity decreases along with increasing UV treatment of algae.

nology. Afterwards, dried, sterilized BaCl_2 crystals are injected by air pressure into the alginate droplets via the crystal gun resulting in an internal polymerization. Final external cross-linking is carried out by a BaCl_2 containing bath (20 mM BaCl_2 , 115 mM NaCl, 5 mM His). After 20 min of incubation, produced alginate capsules are rinsed in 0.9% w/v sterile NaCl solution to remove free barium ions. (Zimmermann, 2003).

Mechanical stability of alginate gels

To determine the relation of the alginate's viscosity to the gel's stiffness, barium-gelled alginate matrices are compressed using a test speed of 0,50 mm/sec at 22 °C and atmospheric pressure.

Modification techniques

First, the alginate's carboxylic groups are activated by 200 mM 1-ethyl-3-(3-dimethylaminopropyl)carbodiimide (EDC) to form an ester after addition of 50 mM N-hydroxysuccinimide (NHS). The obtained alginate-NHS ester is subsequently coupled with streptavidin. Proof of modification is demonstrated via binding of biotin-4-fluorescein and CLSM microscopy.

RESULTS & DISCUSSION

Production of UHV alginates

Since the alginate's chemical composition determines the capsule properties and functionality, a defined and standardized process in terms of the algae's harvest, transport, preparation and final alginate

extraction is essential to obtain UHV alginates with constant quality. Reliable characterizations of growth areas are carried out by determining the geographical location via GPS, water analysis and weather data such as temperature and moisture. The transport of collected algal material is GPS tracked and monitored in respect to exist-

ing temperature and humidity within the UV protective sample container. Gentle preparation and extraction procedures ensure the conservation of the alginate's viscosity. Avoiding material stress during the extraction as far as possible, the impact of acidic treatment on the alginate's viscosity is examined [Figure 1, left]. Acidic treatment of algal material leads to the acidic hydrolysis of glycosidic bonds between the monomer units resulting in reduced chain lengths and thus in low viscosity alginates. As a result, the alginate's viscosity is adjustable due to acidic treatment. Moreover, alginate extractions from fresh algae indicate an increase of the alginate's viscosity compared to algal material subjected to drying processes. Chain fractures may occur due to shrinkage of granular algal material while drying.

Characteristics of UHV alginates and gels

Due to the fact that various conditions such as the growth area, the harvest and the treatment of algae affect the alginate's characteristics, the specification of the polymer's chemical character is crucial in order to understand and control the microcapsule's properties and functionality. The chemical composition and sequential struc-

ture of alginates are obtained using $^1\text{H-NMR}$ spectroscopy. Structural characteristics such as the molecular weight are linked to rheological properties of the polymer solution which are critical for capsule formation. The extracted alginates exhibit high dynamic viscosities (LN: $\eta = 6.0\text{-}9.2$ Pa·s and LT: $\eta = 0.4\text{-}1.6$ Pa·s) as 0.65 % w/v solutions at 20 °C. The viscosity of the applied alginate solution for capsule formation can be adjusted using desired LN:LT ratios. Due to the fact that the biocompatibility of alginate-based capsules is determined by the alginate's purity, sterile alginates are produced with protein contents <40 $\mu\text{g}/\text{ml}$ and bacterial endotoxin values at least <100 Eu/g. Furthermore, mechanical resistance of the capsule material against various forces during an application is essential for its success. Here, increased viscosities result in gel matrices with raised load capacity.

Ultraviolet treatment of algae

In the literature, alginate degradation by direct UV irradiation is well described (Wasikiewicz, 2005), but lacks of information in respect to its behavior in the algal substrates. Therefore, algal material is treated with UV for various durations. Subsequently, extracted alginate solutions are characterized in respect to their dynamic viscosities [Figure 1, right]. The reduction of the alginate's viscosity due to increasing UV irradiation of the algal substrates is demonstrated. The energy input owing to the UV treatment cleaves the alginate chain bondage a) directly and/or b) indirectly via the excitation of plant compounds, e.g. dyestuffs, resulting in the formation of radicals such as peroxide and singlet oxygen. To maintain the original alginate structure and hence its ultra-high viscosity, the protection of collected algae against UV radiation is required and thus UV protective sample container are applied.

UHV alginate modification

To improve the functional performance of the capsule, the alginate structure is modified either by bulk or surface modification. Alginate chains are modified by streptavidin conjugations via carbodiimide chemistry resulting in effective binding sites for versatile biotinylated molecules [Figure 2]. In such a way, the chemical and mechanical stability of the capsule are improved. For instance, crosslinking, bio-com-

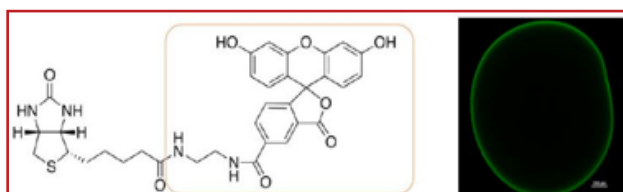


Figure 2: alginate capsule surface modified with streptavidin via carbodiimide chemistry. Streptavidin-coupling is proofed via binding of biotin-4-fluorescein (left) and resulting fluorescence emission demonstrated using confocal laser scanning microscopy (right).

patibility and diffusion properties are adjustable using appropriate biotinylated substances.

CONCLUSIONS

In contrast to common procedures, gentle and well documented methods for alginate production from brown algae LN and LT are presented to maintain original characteristics of extracted UHV alginates for improved capsule performance. Besides favorable chemical and mechanical stability, streptavidin modification of UHV alginates is demonstrated as a promising tool in respect to control the capsule's functionality. Since the viscosity affects cellular behavior, UHV alginates are a promising system for cell encapsulation.

REFERENCES

- de Vos, P., Bučko, M., Gemeiner, P. et al. Multiscale requirements for bioencapsulation in medicine and biotechnology. *Biomaterials* 30, 2559-2570 (2009)
- Zimmermann, H., Ehrhart, F., Zimmermann, D. et al. Hydrogel-based encapsulation of biological, functional tissue: fundamentals, technologies and applications. *Appl. Phys. A* 89, 909-922 (2007)
- Zimmermann, H., Hillgärtner, M., Manz, B. et al. Fabrication of homogeneously cross-linked, functional alginate micro-capsules validated by NMR-, CLSM and AFM-imaging. *Biomaterials* 24, 2083-2096 (2003)
- Wasikiewicz, J. M., Yoshii, F., Nagasawa, N. et al. Degradation of chitosan and sodium alginate by gamma radiation, sonochemical and ultraviolet methods. *Radiat Phys Chem* 73, 287-295 (2005)



Andre Schulz

Fraunhofer IBMT
Medical Technology
St. Ingbert - Germany

andre.schulz@ibmt.fraunhofer.de

INTRODUCTION

Each participant of the 23th International conference on Bioencapsulation was invited to attend the 2014 BRG General Assembly, held in Delft, Netherlands on September 2, 2015

2014 ACTIVITY REPORT

Three issues of the BRG newsletter were published in 2014 under the supervision of Paul de Vos from Groningen University (The Netherlands) and edited by Brigitte Poncelet from Impascience (France). The newsletter is sent by email to 5000 persons.

- April issue was dedicated to the probiotic encapsulation and was managed by André Brodkorb, from Teagasc research center, Ireland.
- July issue presented the contributions from the speakers of the The 17th Industrial Convention on Microencapsulation
- Best student contributions from the 22th International Conference on Bioencapsulation were presented in the October issue

Four events were organized in 2014

- The 6th training School held in Nha-Trang, Vietnam on March 4-7 and co-organized by Agrosuo Dijon and the Nha Trang University
- The 17th Industrial Convention on Microencapsulation, held in Brussels on April 23-25, co-organized by Jean-Paul Simon.
- The 22th International Conference on Bioencapsulation, held in Bratislava, Slovakia on September 17-19, co-organized by Igor Lacik from the Slovak Polymer Institute.
- The 2nd Latin-America Symposium on Encapsulation, held in Joao Pessoa on November 24-26, co-organized by the Federal University of Paraiba.

Table 1 reports the participants and contributions numbers for each event.

2014 FINANCIAL REPORT

The 2014 accounting was externally audited by HPL audit, Nantes, France. A summary of the incomes and expenses is presented in table 2 for each event and the BRG operating. Table 3 presents the cash flow over 2014 itself. Those bring a few remarks :

- All together the cash flow is reduced during 2014 but the final

balance remains highly positive.

- One of the reasons of this decreased balance is linked to the financial crisis that reduced the industrial attendance at Brussels convention (85 participants compared to 96 at Madison 2013 or 124 at Archamps 2012).
- The participation at Bratislava conference was lower than expected but we maintained the number of 50 grants.
- The training school in Vietnam was largely financed by the BRG to support the event.
- The line «External financing» in Table 2 represents external fundings, from the French University Association for the The 6th training School, and from different Brazilian funding organisations for 2nd Latin-America Symposium on Encapsulation. This money didn't pass through the BRG bank account and was used for offering additional grants.
- Each participant who got a grant from the BRG or through external funding got also a free registration that had to be compensated by the BRG.
- As a final remark, the situation seems to be more positive in 2015, and we may finish the year with a cash flow similar to that of 2013.

A report of the annual financial report for 2014 as prepared by HLP auditors and presented to the assembly. The acceptance of this report was moved by Ron Neufeld (Treasurer) and seconded by Paul de Vos. A vote was called and the association unanimously accepted the auditor's report.

BRG GRANTING

Question was bring about the strategy adopted for attributing the BRG grants.

- Registration fees (conference, training school ...) for students and researchers are defined to cover the real cost of their participation and keep as low as possible.
- The financing of the scholarships and grants is provided by the participation of industrials and exhibitors, and in some case through external fundings.
- Non-granted participant DO NOT contribute to the financing of BRG support.

BRG GENERAL ASSEMBLY

- Grants are attributed on merit by the scientific committee, and based on the quality of the contribution (oral or poster), taking into account financial and geographical situation of the participant.
- A substantial part of the BRG support will be attributed in the future to promote participation of groups to the BRG events, i.e. for participation of one professor with several students from the same laboratory, up to 30% registration fees reduction will be applied to the group.

STEERING COMMITTEE

The General Assembly elected the following Steering Committee, until the next General Assembly to be held in September 2016:

- The only nominee for president was Denis Poncelet, and the vote was carried unanimously by the members
- The only nominee for treasurer was Ron Neufeld, and the vote was carried unanimously by the members
- A request for nominations for secretary was presented, and two persons volunteered, Stephane Drusch and Priyanha Tripathy from India. A vote was called, and those persons were conjointly elected.
- Paul De Vos was elected as co-president and newsletter chief-editor, with support from Brigitte Poncelet

The Steering Committee will be completed with the local organizers of the 2016 events.

Table 1	Participants					Contributions		Grants
	Indus-trials	Resear-chers	Stu-dents	Exhi-bitors	Total	Orals	Pos-ters	
Nha Trang	5	45	17	-	67	16	17	51
Brussels	52	14	-	19	85	12	-	12
Bratislava	10	55	50	4	119	40	51	51
Joao Pessoa	12	56	60	3	131	27	65	44

2015-2016 ACTIVITIES

Three events were organized in 2015:

- 7th training School on Bioencapsulation, Strasbourg, France, February 23-26, 2015
- 18th Microencapsulation Industrial Convention, Eindhoven, The Netherlands, February 22-24, 2015
- 23th International Conference on Bioencapsulation, Delft, Netherlands, September 2-4, 2015

Three events are already scheduled for 2016:

- 19th Microencapsulation Industrial Symposium to be held in Frankfurt, Germany, April 4-6, 2016, co-organized by Thorsten Brandau from BRACE GmbH.
- 8th Training School on Bioencapsulation, to be held in Cork, Ireland, May 30-june 2, 2016, and co-organized by André Brodtkorb from Teagasc Food Research Center.
- 24th International Conference on Bioencapsulation, to be held in Lisbon, Portugal, September 21-23, 2016, co-organized by Catarina Pinto Reis from Universidade Lusofona.

Some proposals have been received to organize meetings in Malaysia (Conference), USA (Convention) or Chile (Conference) in 2017.

Four newsletter issues have been or will be published in 2015 :

- The January issue was edited by Thierry Van damme from Strasbourg University, France, on Drug targeting and encapsulation
- The May issue was dedicated to the ITN Powtech (Particle and powder technologies)
- The July issue was edited by Raul Rodrigo Gomez from P&G, on Industrial application of micro encapsulation
- This issue presents the 2015 Poncelet award and the ten best student contributions from the 23th International Conference on Bioencapsulation

Four newsletter issues are already scheduled for 2016 :

- In January, a part II on Industrial applications of microencapsulation
- In may, microencapsulation in agriculture
- In july, the topic has to be finalized
- in October, the best contributions XXIV International Conference on Bioencapsulation from

CLOSING

As no question was raised by the participants, the General Assembly was closed by the President.

Table 2 : Conference and BRG operating budget 2014						
	Nha_trang	Brussels	Bratislava	Joao_Pessoa	BRG	Total
registration	5094 €	94 900 €	37 146 €	20 357 €	1825 €	159 322 €
Interests					536 €	536 €
Receptions	-407 €	-59 242 €	-21 882 €	-9 268 €	-939 €	-91 738 €
Printing/mailling		-11 770 €	-3 583 €	-353 €	-	-15 316 €
Management	-9240	-13 770 €	-6 622 €	-9 240 €	-2160 €	-41 032 €
Grants-Missions	-14 926 €	-3011 €	-23 300 €	-4 175 €	-1000 €	-46 412 €
Bank costs	81 €	-934 €	-583 €	-517 €	-178 €	-2131 €
Divers			-54 €	-23	-183 €	-260 €
Balance	-19 398 €	6563 €	-18 878 €	-3219 €	-2099 €	-37 031 €
External financing	20 000 €			25 000 €		45 000 €
Free registration	14 500 €		15 000 €	7000 €		36 500 €

« Grants » corresponds to support offer participants for their travel and accommodation, « Missions » corresponds to the reimbursement of the speakers or chairperson, external financing is funding that has been spend for offering additional grants, all grants and missions get free registration which has to be compensate by BRG.

Table 3 : cash flow over 2014	
End of 2013 balance	79 321 €
2014 Nha Trang	-15 078 €
2014 Brussels	16 275 €
2014 Joao Pessoa	-11 977 €
2014 Bratislava	-18 227 €
2015 Eindhoven	-2 668 €
2015 Strasbourg	4 001 €
2015 Delft	-392 €
2014 BRG	-1 947 €
Solde end of 2013	49 308 €



114 Allée Paul Signac,
44240 Sucé sur Erdre
France
contact@bioencapsulation.net

Bioencapsulation Research Group is a non-profit association promoting networking and research in the encapsulation technology of bioactives. It organises academic conferences and industrial symposiums, publishes newsletters and manages a website.

More information : <http://bioencapsulation.net>

KEEP CONTACT BY REGISTERING ...

Registration is based on a voluntary annual fee. If you wish to simply receive the newsletter and be advised about future events, register online at: <http://bioencapsulation.net>

Be an active member pay the registration fee and get more services

- Reduced registration fees to BRG events
- Full access to conference proceedings (> 1700)
- Access to the forum and internal mailing
- Possibility to contribute to the newsletter
- Reduction for the conference registration
- Priority for awarding of conference grants

Class	Annual fees
Industry members	100 €
Researchers ¹	60 €
Students ²	Free
Honorary member and corporate registration ³	1000 €

¹ public and non-profit organizations, contact us for group registration

² registered for a master or PhD program, less than 30 years old.

³ Open access to 1 full page in 1 issues (1/2 page in 2 issues ...) in the newsletter
Registration fees may be paid by credit card, bank transfer or cheque.

For more information or an invoice, see the registration page on <http://bioencapsulation.net>

Thanks to **Agence I** (<http://www.agence-i.eu/>) for designing the newsletter., Brigitte Poncelet (<http://im-pascience.eu>) editing corrections and the editorial board for their help.

STEERING COMMITTEE

- **Prof. Denis Poncelet**, Oniris, France (President)
- **Prof. Stephan Drusch**, TU Berlin, Germany (Secretary)
- **Mrs Priyanha Tripathy**, CSIR, India (Secretary)
- **Prof. Ronald J. Neufeld**, Queen's University, Canada (Treasurer)
- **Prof. Paul De Vos**, Groningen University, Netherlands (Newsletter editor)

- **Dr. Micheal Whelehan**, Solvotrin, Ireland
- **Dr André Brodkorb**, Teagasc Food Research Centre, Ireland (Editor)
- **Dr Thorsten Brandau**, Brace GmbH, Germany [Industrial contact]
- **Prof. Elena Markvicheva**, Institute of Bioorganic Chemistry, Russia
- **Prof Luis Fonseca**, Instituto Superior Técnico, Portugal
- **Prof. Harald Stover**, McMaster University, Canada
- **Dr James Oxley**, SwRI, USA
- **Prof. Igor Lacik**, Polymer Institute, Slovakia
- **Dr Nicole Papen-Botterhuis**, TNO, Netherlands
- **Dr Gabriele Meester**, DSM, Netherlands
- **Dr Amos Nussinovitch**, Hebrew University, Israel
- **Prof Gary Reineccius**, University of Minnesota, USA
- **Dr Corinne Hoesli**, McGill University, Canada
- **Dr Laura Hermida**, NITI, Argentina
- **Mr Luis Roque**, Univ. Lusofona, Spain
- **Mrs Catarina Silva**, S Univ. Lusofona, Spain.

REGISTRATION DATA

- Title:
- First name: Last name:
- Affiliation: Department:
- Address: Address (cont.):
- Zipcode: City:
- State: Country:
- Phone: Fax:
- Email: Website:
- Password: Repeat password:
- Registration class: Registration fees: €

Send your registration to : Bioencapsulation Research Group 114 Allée Paul Signac, 44240 Sucé sur Erdre France